Field Guides

Paleogene calderas of central and eastern Oregon: Eruptive sources of widespread tuffs in the John Day and Clarno Formations

Jason D. McClaughry, Mark L. Ferns, Martin J. Streck, Karyn A. Patridge and Caroline L. Gordon

Field Guides 2009;15;407-434
doi: 10.1130/2009.fld015(20)

The Geological Society of America
Field Guide 15
2009

Paleogene calderas of central and eastern Oregon: Eruptive sources of widespread tuffs in the John Day and Clarno Formations

Jason D. McClaughry*
Mark L. Ferns
Oregon Department of Geology and Mineral Industries, 1995 3rd Street, Baker City, Oregon 97814, USA

Martin J. Streck
Department of Geology, Portland State University, Portland, Oregon 97207, USA

Karyn A. Patridge
School of Earth & Environmental Sciences, Washington State University, Pullman, Washington 99164, USA

Caroline L. Gordon
Ochoco National Forest, 3160 NE 3rd Street, Prineville, Oregon 97754, USA

ABSTRACT

The John Day Formation of central and eastern Oregon, contains a widespread assemblage of both ash-flow and airfall tuffs, yet only a few corresponding caldera sources have been identified in the region. Investigators have long speculated on the sources of tuffs in the John Day Formation and have suggested that these pyroclastic rocks were vented from now buried eruptive centers in or marginal to a nascent Cascade Range. Recent detailed geologic mapping in the John Day and Clarno Formations, however, indicates the presence of at least three large-scale rhyolite caldera complexes centered along the northeast-trending axis of the Blue Mountains. This field guide describes a three-day geologic transect, from the scenic high desert of central Oregon eastward across the axis of the Blue Mountains, that will examine the physical volcanology and geologic setting of the 41.50–39.35 Ma Wildcat Mountain caldera exposed along the crest of the Ochoco Mountains, the 29.56 Ma Crooked River caldera at Prineville, and the 29.8 to 28.1 Ma Tower Mountain caldera near Ukiah.

INTRODUCTION

Calderas that result from the collapse of a central vent area during voluminous pyroclastic eruptions have until recently been relatively unknown in the Paleogene geologic record of Oregon. Defined by regional geologic mapping three Paleogene calderas have now been identified across central and eastern Oregon: (1) the 41.50–39.35 Ma Wildcat Mountain caldera exposed along the crest of the Ochoco Mountains, (2) the 29.56 Ma Crooked River caldera at Prineville, and (3) the 29.8 to 28.1 Ma Tower Mountain caldera near Ukiah in northeast Oregon (Fig. 1) (Ferns et al., 2001; McClaughry and Ferns, 2007). Geologic mapping

*jmcclaughry@dogami.state.or.us

McClaughry, J.D., Ferns, M.L., Streck, M.J., Patridge, K.A., and Gordon, C.L., 2009, Paleogene calderas of central and eastern Oregon: Eruptive sources of widespread tuffs in the John Day and Clarno Formations, *in* O'Connor, J.E., Dorsey, R.J., and Madin, I.P., eds., Volcanoes to Vineyards: Geologic Field Trips through the Dynamic Landscape of the Pacific Northwest: Geological Society of America Field Guide 15, p. 407–434, doi: 10.1130/2009.fld015(20). For permission to copy, contact editing@geosociety.org.

suggests two additional Oligocene to early Miocene calderas in the southwest Oregon Cascades, but these have yet to be fully mapped (Fig. 1; Hladky and Wiley, 1993; Hladky, 1996). The apparent lack of Paleogene calderas in Oregon is a noteworthy anomaly considering that numerous Paleogene calderas have been mapped in adjacent Idaho (McIntyre et al., 1982; Leonard and Marvin, 1982; Moye et al., 1988) and many more have been identified further south in volcanic fields of the Great Basin (Steven and Lipman, 1976; Ludington et al., 1996).

The Wildcat Mountain, Crooked River, and Tower Mountain calderas are part of a broad sweep of voluminous ash-flow tuff magmatism (ca. 41–23 Ma) preserved in volcanic and intrusive rocks distributed across the axis of the Blue Mountains in central and eastern Oregon (Walker and Robinson, 1990; Robinson et al., 1990) and in correlative rocks extending into the Western Cascades in southwest Oregon (Retallack et al., 2004), at Hart Mountain in south-central Oregon (Mathis, 1993), and near Potlatch in northern Idaho (Kauffman et al., 2003)(Fig. 1). Regionally, these igneous centers may represent a northward extension of the contemporaneous middle Eocene to Oligocene (ca. 43–23 Ma) "ignimbrite flare up" in the Great Basin of the southwest United States (Stewart and Carlson, 1976; Best et al., 1989; Christiansen and Yeats, 1992; Ludington et al., 1996; Honn and Smith, 2007). In central and eastern Oregon, this magmatic episode is recorded in the Eocene Clarno and middle Eocene to early Miocene John Day Formations, which cover an area exceeding 30,000 km^2 (Fig. 1)(Swanson, 1969; Robinson, 1975; Robinson and Brem, 1981; Robinson et al., 1984, 1990; Smith et al., 1998). Rocks of the Oligocene Tower Mountain and Crooked River calderas are part of the John Day Formation. Older rocks of the middle Eocene Wildcat Mountain caldera record part of a regional transition from dominantly calc-alkaline magmatism that characterizes the Clarno Formation to the bimodal basalt and rhyolite volcanic assemblage associated with the John Day Formation.

Regional workers have long speculated on the sources of tuffs in the John Day Formation (Robinson et al., 1984, 1990) and have suggested that pyroclastic rocks within the formation were vented from now-buried eruptive centers in or marginal to an antecedent Cascade Range. These presumed buried sources were used to build a tectonic model in which John Day volcanism documented a westward jump of an Eocene subduction zone at the end of "Clarno arc" volcanism (Coleman, 1949; Robinson et al., 1984, 1990; White and Robinson, 1992, Bestland et al., 1999). From volume estimations of ash-flow tuffs within the formation, Robinson et al. (1990) concluded that such eruptions would not have resulted in collapse calderas. Therefore, small inlier Oligocene rhyolite domes at Powell Buttes, Grizzly Mountain, and Juniper Butte were suggested as eruptive sites (Swanson, 1969; Robinson et al., 1984, 1990) as well as the Smith Rock-Gray Butte area (Obermiller, 1987; Smith et al., 1998). Recent detailed geologic mapping in the region has identified the Wildcat Mountain, Crooked River, and Tower Mountain calderas as volcanic vents much larger than the small, isolated eruptive centers envisaged by preceding workers. These newly recognized calderas and their correspondent ash-flow and airfall tuff deposits distributed well east of previously postulated vent areas document a regionally extensive magmatic episode unrelated to an inferred ancestral Cascade Range.

OBJECTIVES OF THIS FIELD TRIP

This field trip guide is for a three-day geologic excursion that will explore aspects of the physical volcanology and geologic

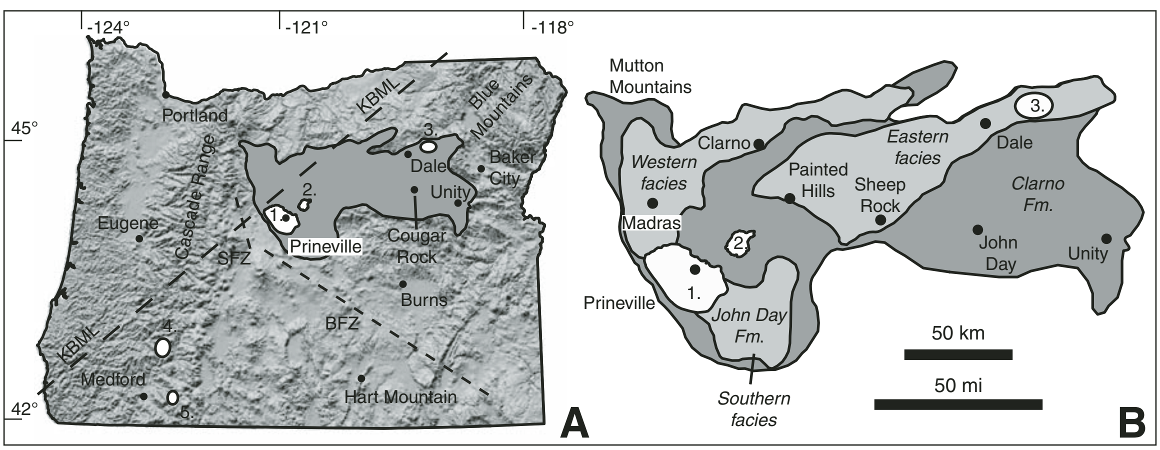

Figure 1. (A) Location of known Paleogene calderas in Oregon. White-filled polygons are calderas: 1—Crooked River caldera, 2—Wildcat Mountain caldera, 3—Tower Mountain caldera, 4 and 5—unnamed, suggested calderas. Light-gray shade represents the approximate distribution of the Eocene to Oligocene Clarno and John Day Formations. Dashed black line labeled KBML is the inferred trace of the Klamath–Blue Mountain gravity-anomaly lineament. Dashed black lines labeled SFZ and BFZ show the general trace of the Sisters and Brothers Fault Zones, respectively. (B) Enlarged central part of A shows the distribution of the "western," "southern," and "eastern" facies of the John Day Formation after Robinson et al., (1990). Select geographic points are shown for reference.

setting of the three Paleogene calderas exposed along the axis of the Blue Mountains (Fig. 2). Field stops within the Crooked River caldera (Day 1), the Wildcat Mountain caldera (Day 2), and the Tower Mountain caldera (Day 3) will examine voluminous ash-flow tuff deposits and post-collapse rhyolite domes associated with each respective eruptive center. Field stops within the Painted Hills and Sheep Rock Units of the John Day Fossil Beds National Monument on Day 2 will provide the opportunity to examine tuffs that punctuate the well-exposed fossil bearing sedimentary sections.

GEOLOGIC SETTING AND REGIONAL PALEOGENE STRATIGRAPHY

Deformed Paleozoic to Mesozoic accreted terranes and Cretaceous marine rocks form the core of the Blue Mountains which are blanketed by a discontinuous succession of Paleogene volcanic and volcanogenic sedimentary rocks referred to as the Clarno and John Day Formations (Fig. 1). The older Clarno Formation consists of Eocene non-marine alkaline to calc-alkaline volcanic rocks and intrusions and volcanogenic sedimentary rocks that reputedly range in age from ca. 54 to 39 Ma (Fig. 3; Merriam, 1901a, 1991b; Evernden et al., 1964; Evernden and James, 1964; Swanson and Robinson, 1968; Swanson, 1969; McKee, 1970; Enlows and Parker, 1972; Rogers and Novitsky-Evans, 1977; Manchester, 1981; Fiebelkorn et al., 1982; Vance, 1988; Walker and Robinson, 1990; Bestland et al., 1999; Retallack et al., 2000; Appel, 2001). A regional stratigraphy has not been established for the Clarno Formation, but available $^{40}Ar/^{39}Ar$ dates obtained from exposures in north-central Oregon form a tightly constrained cluster of ages for intermediate calc-alkaline rocks that range between 43.86 ± 0.89 and 41.50 ± 0.48 Ma (Bestland et al., 1999; Appel, 2001; Ferns and McClaughry, 2007). Urbanczyk (1994) identified a similar aged (43.5 ± 0.4 to 36.7 ± 0.2 Ma) magmatic pulse in rocks correlative with the Clarno Formation at Cougar Rock in the Elkhorn Mountains of eastern Oregon and a secondary pulse that occurred between 37.6 ± 0.4 and 33.6 ± 0.3 Ma. A suite of older rocks, that range in age from 53.6 ± 0.3 to 45.26 ± 0.31 Ma, similar to the Challis volcanic field of Idaho (ca. 51–44 Ma; McIntyre et al., 1982) are exposed near the hamlets of Clarno and Mitchell (Bestland et al., 1999; Appel, 2001). These rocks are inferred to mark the lower boundary of the Clarno Formation in north-central Oregon, although the precise stratigraphic relationships of these older units is not clear.

The John Day Formation is a dissected belt of late Eocene to late Oligocene volcanogenic sedimentary rocks, mafic lavas, rhyolite domes, and widespread rhyolite tuffs originally thought to be entirely younger than and chemically distinct from the Clarno Formation (Fig 3; Marsh, 1875; Peck, 1964; Swanson, 1969; Fisher and Rensberger, 1972; Robinson, 1975; Robinson and Brem, 1981; Robinson et al., 1984, 1990; Obermiller, 1987). The regional stratigraphy of the John Day Formation was established by Peck (1964), Fisher and Rensberger (1972), Robinson

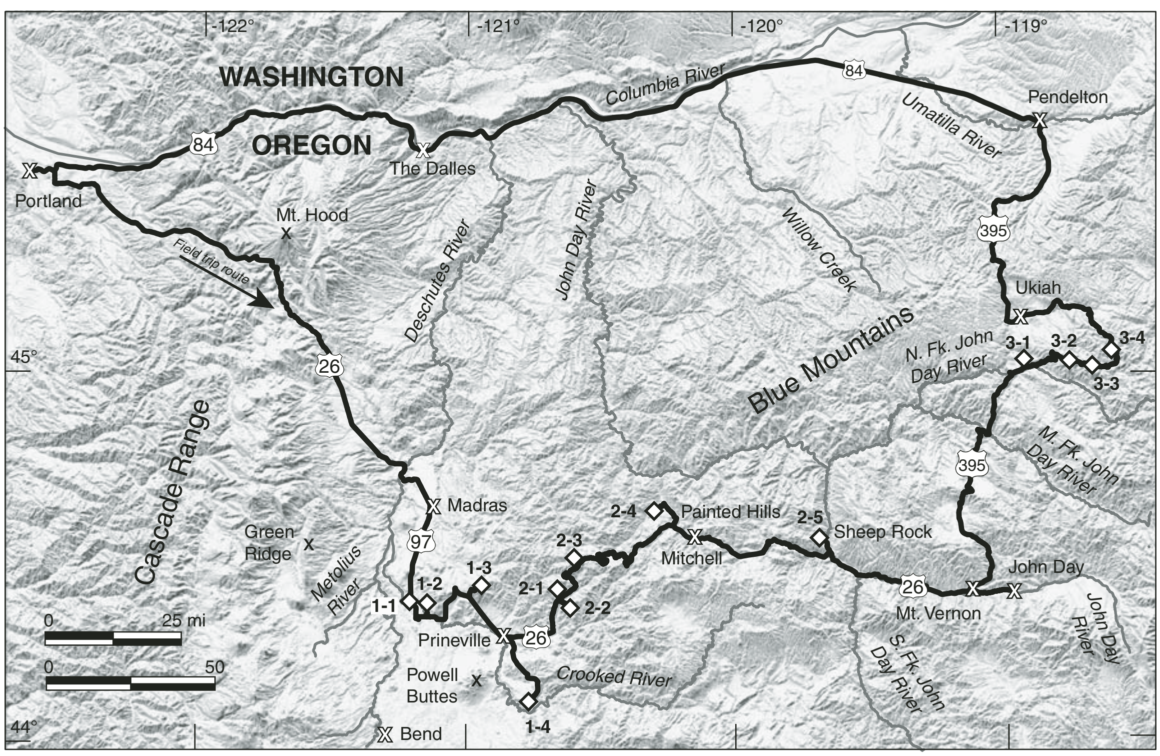

Figure 2. Sketch map showing the field trip route and the locations of numbered field stops referred to in the text.

and Brem (1981), and Robinson et al. (1990). Robinson and Brem (1981) divided the formation into a "western," "southern," and "eastern" facies (Fig. 1). The "western" facies is divided into members designated alphabetically from A to I (Fig. 3) (Peck, 1964; Robinson and Brem, 1981; Robinson et al., 1990). The "eastern" facies is divided into four members that include from oldest to youngest the Big Basin, Turtle Cove, Kimberly, and Haystack Valley Members (Fig. 3) (Fisher and Rensberger, 1972). The "southern" facies has not been formally divided into members. The base of the John Day Formation is defined by the regionally widespread Member A ash-flow tuff, which has returned single crystal $^{40}Ar/^{39}Ar$ ages of 39.72 ± 0.03 Ma near the Painted Hills, 39.22 ± 0.03 Ma near Clarno, and 39.17 ± 0.15 Ma near Ashwood (Fig. 3; Bestland and Retallack 1994a, 1994b; Smith et al., 1998; Retallack et al., 2000). An ash-flow tuff, defined as Member I near the top of the formation has been dated at 27.7 ± 0.3 Ma (K/Ar), but may be as young as 22 Ma (?) (Robinson et al., 1990).

DAY 1. THE CROOKED RIVER CALDERA

Day 1 of this field trip will examine the Oligocene Crooked River caldera, the largest of the three Paleogene calderas. Eruption of the Tuff of Smith Rock at 29.56 Ma resulted in the formation of the Crooked River caldera, a 41 km × 27 km volcano-tectonic depression, whose partially eroded remains underlie the western half of the Lower Crooked Basin between Prineville and Redmond in central Oregon (Fig. 4). The semi-elliptical, northwest-southeast elongated subsidence area of the caldera extends from Gray Butte on the northwest, along the western front of the Ochoco Mountains, and southeast nearly to Prineville Reservoir. It is drained by the through-flowing Crooked River, for which the structure is named, and the tributaries of Ochoco Creek and McKay Creek.

The Crooked River caldera is the major vent feature of the Lower Crooked volcanic field, a bimodal basalt and rhyolite assemblage within the John Day Formation that covers more than 1500 km^2. Mafic rocks within the Lower Crooked volcanic field are tholeiitic, with enriched FeO and TiO_2 contents and relatively low amounts of Al_2O_3 (Fig. 5; Table 1). Silicic rocks in the Lower Crooked volcanic field are characterized by elevated abundances for the incompatible high-field strength elements Ba, Zr, Nb, and generally have higher abundances for Y and the light rare earth elements La and Ce (Fig. 5; Table 1).

The Lower Crooked volcanic field lies within a relatively undissected structural area juxtaposed between the Klamath–Blue

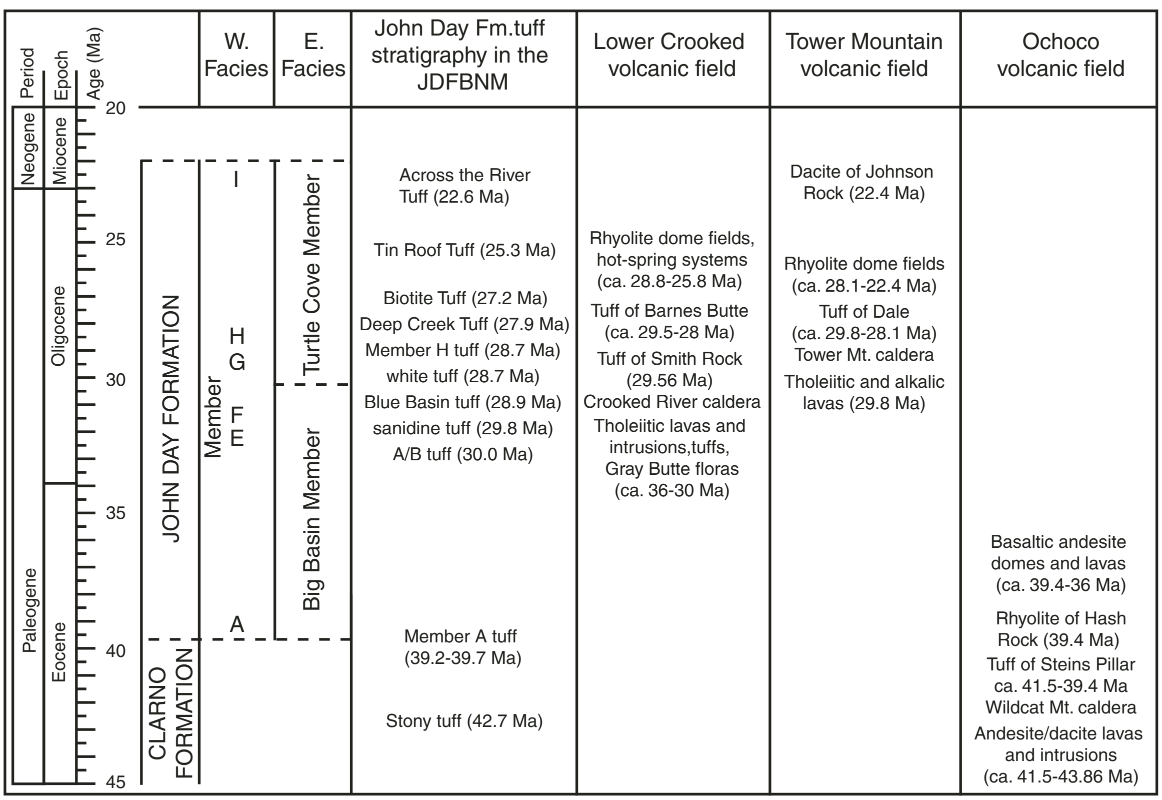

Figure 3. Regional stratigraphy of the John Day and Clarno Formations in the John Day Fossil Beds National Monument (JDFBNM) and temporally correlative Paleogene volcanic fields in central and eastern Oregon. Radiometric age-dates for tuffs in the John Day and Clarno Formations are from (Bestland, 1995; Smith et al., 1998; Bestland et al., 1999; Retallack et al., 2000; Albright et al., 2008).

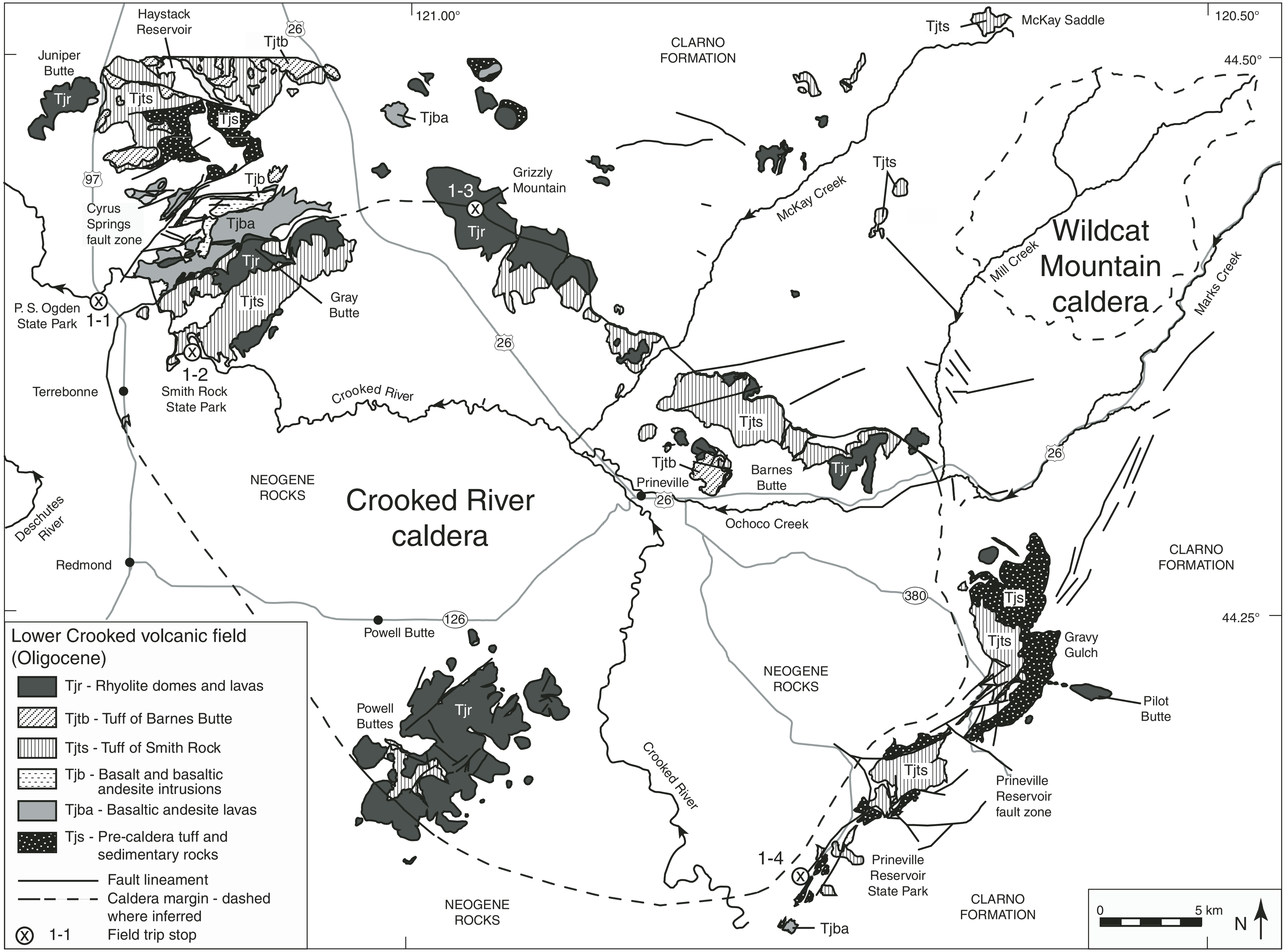

Figure 4. Simplified geologic map of the Crooked River caldera labeled with associated field stops.

Mountain gravity-anomaly lineament (Riddihough et al., 1986) and junction of the Brothers and Sisters fault zones (Fig. 1). Two major fault zones that parallel the northeast trend of the Klamath–Blue Mountain gravity-anomaly lineament bracket the caldera. The Cyrus Springs fault zone (Smith et al., 1998) bounds the northwest margin while the Prineville Reservoir fault zone bounds the southwest margin. These faults define a circumferential, peripheral fault zone that mimics the arcuate structural margin of the caldera. This peripheral fault zone extends at least 10 km outside the main area of subsidence and is associated with numerous small rhyolite intrusions (Fig. 4).

Magmatism in the Lower Crooked volcanic field progressed through five stages. The earliest eruptions produced a series of Fe- and Ti-rich tholeiitic basaltic andesite and andesite lavas compositionally similar to icelandite that erupted from volcanic centers between Haystack and Prineville Reservoirs between ca. 36 and 30 Ma. Eruption of the voluminous Tuff of Smith Rock accompanied the major subsidence phase of the Crooked River caldera at 29.56 Ma. Subsequently, the tuff of Barnes Butte erupted between ca. 29.56 and 27.97 Ma from a now obscure vent source in the southeast part of the Crooked River caldera. Following major ash-flow tuff eruptions, a series of large (20–80 km^2) rhyolite dome and flow fields were emplaced along the structural margin of the caldera up to ca. 25.8 Ma, when major volcanic activity in the field ceased. Rhyolite domes and lavas are prominently exposed at Powell Buttes (28.3 ± 1.0, K/Ar, anorthoclase, Evans and Brown, 1981; 25.8 ± 0.2 Ma; K/Ar, sanidine, Robinson et. al, 1990), Gray Butte (28.82 ± 0.23 Ma, $^{40}Ar/^{39}Ar$, anorthoclase, Smith et al., 1998), Grizzly Mountain (no age data), Barnes Butte (27.97 ± 0.32 Ma, $^{40}Ar/^{39}Ar$, whole rock, McClaughry and Ferns, 2006a), Ochoco Reservoir (27.54 ± 0.36 Ma, $^{40}Ar/^{39}Ar$, whole rock, McClaughry and Ferns, 2006b), and Pilot Butte (no age data) (Fig. 4). Hotsprings formed during the post-subsidence phase both within and around the periphery of the caldera. Hydrothermal systems deposited massive quartz and calcite veins (± cinnabar) along the ring-fracture and peripheral fault structures as well as finely laminated to massive mudstones, siliceous pool sinter, and sinter breccia along the caldera margin.

Rocks of the Crooked River caldera straddle a stratigraphic discontinuity between the "western" and "southern" facies of the John Day Formation; tuffs erupted from the caldera are correlative with Members G and H of Peck (1964) and Robinson (1975) (Fig. 3). The Tuff of Smith Rock, correlative with Member G of the "western" facies, has returned $^{40}Ar/^{39}Ar$ radiometric age-date determinations of 29.53 ± 0.09 Ma and 29.57 ± 0.17 Ma at Haystack Reservoir ($^{40}Ar/^{39}Ar$, sanidine, Smith et al., 1998) and 29.56 ± 0.17 Ma ($^{40}Ar/^{39}Ar$, feldspar) at McKay Saddle. These dates are indistinguishable from geochemically similar John Day Formation Member G tuffs (Table 1) exposed north of the Crooked River caldera that have $^{40}Ar/^{39}Ar$ ages of 29.61 ± 0.10 west of Teller Flat and 29.54 ± 0.10 Ma near Antelope ($^{40}Ar/^{39}Ar$, alkali feldspar, Smith et al., 1998). The Tuff of Barnes Butte, erupted around 28.5 Ma, is stratigraphically correlative with Member H exposed in the "western" facies and within the Turtle Cove Member of the "eastern" facies (Peck, 1964; Robinson, 1975). Smith et al. (1998) report an $^{40}Ar/^{39}Ar$ age of 27.62 ± 0.63 Ma ($^{40}Ar/^{39}Ar$, sanidine) for a tuff they correlate with Member H in the western facies exposed at Haystack Reservoir. Retallack et al. (2000) reports single crystal $^{40}Ar/^{39}Ar$ ages of 28.65 ± 0.05 Ma and 28.65 ± 0.07 Ma for the Member H tuff capping Carroll Rim in the "eastern" facies (Fig. 3).

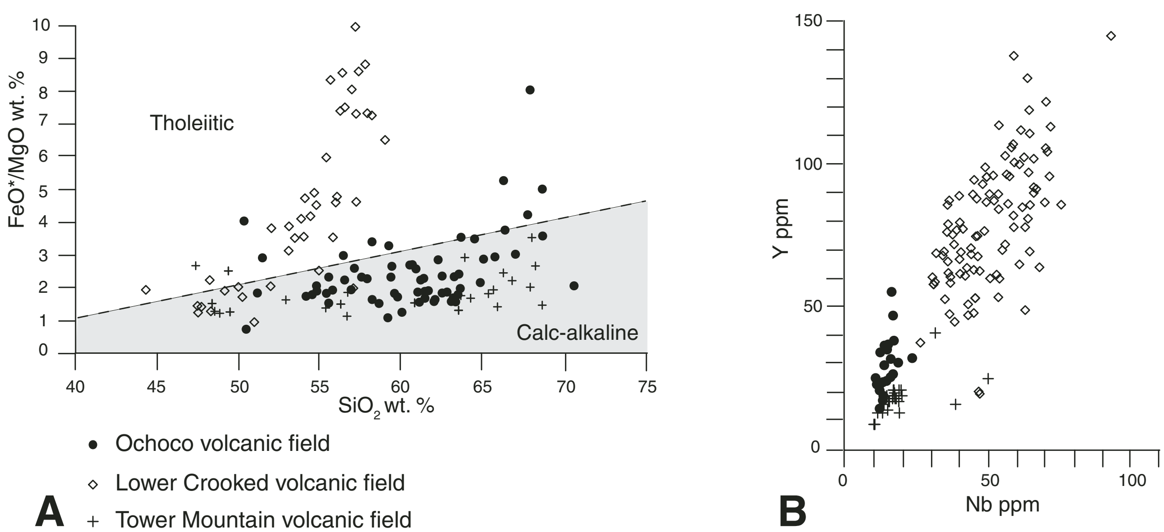

Figure 5. Variation diagrams for whole-rock geochemical analyses from the Ochoco, Lower Crooked, and Tower Mountain volcanic fields. (A) FeO*/MgO versus SiO_2 diagram showing differences between mafic to intermediate rocks within the three volcanic systems. Tholeiitic and calc-alkaline fields are from Miyashiro (1974). (B) Plot of Y versus Nb for silicic rocks within the three volcanic systems.

TABLE 1. WHOLE-ROCK GEOCHEMICAL ANALYSES OF SELECTED ROCKS FROM THE LOWER CROOKED VOLCANIC FIELD AND CROOKED RIVER CALDERA

	Pre-caldera rocks				Tuff of Smith Rock						Post-caldera rhyolite domes and flows									
	Tuff of Eagle Rock	Tuff of Antelope Creek	Basaltic andesite	Basalt	Intra-caldera tuff	Outflow tuff														Tuff of Barnes Butte
Sample number:	18 LC 06	PAT PR11	16 LC 06[†]	RC95-76[§]	24 LCJ 06	22 LCJ 06	448 LCJ 07	394 LCJ 07	PAT TF1	PH95 376[†]	95-BE-31[#]	RC95-70B[§]	PAT GR1	08-PJ-05	7.29VI. 05	15 P 05	1.15VII. 05	520 LCJ 08	PAT BB1	PAT OR2A
Geographic area:	Prine-ville Res.	Prine-ville Res.	Prine-ville Res.	Gray Butte	Smith Rock	Owl Creek	McKay Saddle	Haystack Res.	Teller Flat	Ante-lope	Juniper Butte	Gray Butte	Grizzly Mt.	Powell Buttes	Powell Buttes	Powell Buttes	Ochoco Res.	Pilot Butte	Barnes Butte	Ochoco Res.
UTM N:	4889220	4888930	4889168	4917728	4914036	4902169	4932290	4928481	4945844	4969320	4926158	4919692	4922320	4897123	4894249	4890217	4908454	4898960	4910352	4906892
UTM E:	680850	680285	680322	647398	648479	688720	687550	646612	661269	669430	641646	651261	662943	663910	662320	660600	682626	691900	674100	681043
Age (Ma):	32.1	ca. 30	ca. 30	ca. 30			29.56	29.57	29.61	29.54		28.82		28.30	25.80		27.54		27.97	
SiO_2	78.97	76.46	55.39	49.99	76.67	77.79	76.25	78.11	76.65	75.21	78.60	76.83	77.87	79.26	74.93	76.23	75.74	78.36	78.05	78.18
Al_2O_3	10.96	11.51	14.16	15.52	12.06	11.57	13.02	10.84	11.50	12.81	10.92	12.40	11.99	11.55	11.62	8.69	11.92	11.80	11.27	11.61
TiO_2	0.18	0.29	2.00	2.58	0.24	0.14	0.24	0.15	0.29	0.32	0.13	0.25	0.22	0.14	0.28	0.33	0.28	0.16	0.16	0.15
FeO*	2.06	3.55	13.56	11.84	2.76	1.81	1.25	1.92	2.80	2.20	1.63	1.31	1.35	1.06	4.24	7.14	3.17	1.03	1.80	1.15
MnO	0.02	0.08	0.27	0.20	0.05	0.02	0.02	0.03	0.04	0.03	0.01	0.01	0.01	0.01	0.04	0.21	0.05	0.01	0.02	0.01
CaO	0.29	0.90	6.08	10.14	0.48	0.16	0.50	0.10	0.29	0.77	0.12	0.37	0.18	0.09	0.29	0.13	0.19	0.13	0.14	0.17
MgO	0.15	0.18	2.26	5.84	0.23	0.16	0.13	0.11	0.05	0.57	0.16	0.10	0.02	0.05	0.14	0.11	0.09	0.09	0.09	0.08
K_2O	3.87	3.48	1.60	0.37	4.24	4.57	4.11	8.40	5.00	6.01	5.01	4.31	4.36	4.32	4.68	4.46	4.55	4.21	5.98	4.95
Na_2O	3.42	3.50	3.74	2.90	3.21	3.62	4.43	0.33	3.32	2.05	3.41	4.39	3.93	3.49	3.72	2.64	3.96	4.15	2.47	3.64
P_2O_5	0.07	0.04	0.92	0.63	0.07	0.05	0.05	0.02	0.06	0.03	0.03	0.03	0.06	0.04	0.05	0.05	0.05	0.05	0.02	0.06
LOI	1.59	3.57	2.70	**N.D.	2.10	0.97	0.92	2.03	1.98	6.84	**N.D.	**N.D.	2.08	0.70	1.67	1.18	0.44	0.81	3.20	2.30
Ni	7	2	4	49	2	5	0	0	0	16	9	15	1	2	6	3	4	1	7	0
Cr	0	1	7	157	0	0	1	1	6	4	0	8	2	0	0	0	0	7	4	2
Sc	2	4	30	34	3	2	3	0	4	4	0	5	3	1	1	0	3	7	1	2
V	13	11	148	280	9	13	14	17	32	8	4	3	0	8	10	32	9	12	14	4
Ba	960	974	374	367	1035	604	1120	111	416	221	309	905	994	963	516	250	765	975	503	520
Rb	118	84	45.7	7.0	134.3	134.9	130.8	180.0	155.4	192.0	179.0	132.0	128.4	115.0	111.9	136.3	118.0	133.3	134.8	124.4
Sr	43	122	291	329	43	19	47	8	18	28	14	46	40	10	17	15	29	18	13	11
Zr	490	484	243	186	512	384	596	420	583	582	373	519	546	462	826	1185	771	455	335	341
Y	120.2	76.3	61.1	40.0	113.7	61.4	113.2	89.6	89.5	103.0	99.0	64.0	86.2	63.1	105.7	145.0	110.8	85.9	66.8	69.3
Nb	64.7	35.6	20.9	23.0	53.8	53.0	71.9	53.6	44.7	56.0	49.0	68.0	57.0	45.0	70.2	93.1	64.6	75.6	40.0	40.5
Ga	23.7	24.6	24.9	19.0	21.6	24.1	25.9	29.7	24.5	28.0	30.0	27.0	25.3	23.0	29.3	30.9	25.1	20.5	21.0	22.9
Cu	0	1	4	46	0	0	0	5	6	7	2	3	2	0	5	7	3	2	5	4
Zn	131	126	120	101	180	115	168	124	122	110	111	135	115	43	155	159	128	50	99	93
Pb	2	10	2	**N.D.	7	8	8	28	14	17	14	16	14	3	11	22	11	1	11	12
La	68	45	29	**N.D.	59	59	68	60	61	**N.D.	81	**N.D.	71	30	68	93	87	96	54	54
Ce	148	78	59	**N.D.	139	128	172	108	134	**N.D.	130	**N.D.	146	68	155	197	186	200	103	111
Th	16.0	7.8	3.2	4.0	18.7	13.7	16.1	20.3	16.4	20.0	15.0	18.0	16.2	12.0	13.3	17.0	14.4	15.2	12.4	14.9
U	5	3	0	**N.D.	5	5	5	5	4	**N.D.	**N.D.	18	3	5	2	1	5	3	4	5
Co	1	0	31	**N.D.	0	0	0	0	**N.D.	**N.D.	**N.D.	0	**N.D.	0	4	10	1	1	0	0

Note: Major element determinations have been normalized to a 100% total on a volatile-free basis and recalculated with total iron expressed as FeO*. Oxides as weight percent; trace elements as parts per million.

[†]Hammond (2008)

[§]Smith et al. (1998)

[#]Smith et al. (1996)

**N.D. = no data or element not analyzed.

Stop 1-1. Northwest Margin of the Crooked River Caldera at Peter Skene Ogden State Park [Global Positioning System (GPS) coordinates –121.1928, 44.3929]

The ridge visible on the east, from the highway bridge at Peter Skene Ogden State Park, is underlain by a southeast-dipping section of middle Eocene to middle Oligocene rocks that form part of the remnant northwestern wall of the Crooked River caldera (Fig. 6). This structural block dips 28°–45° southeast, back toward the interior of the caldera where it is abruptly terminated by the primary caldera bounding ring-fault. The base of the section is composed of calc-alkaline basalts and basaltic andesites of the Clarno Formation. These lavas are overlain by the John Day Formation, which here includes Fe- and Ti-rich basalts and andesites, interbedded volcaniclastic sedimentary rocks, and ash-flow tuff. The volcaniclastic sedimentary rocks in this section host the well-known Gray Butte fossil floras including the Kings Gap, Sumner Spring, Nichols Spring, Canal, and Trail Crossing floras. These floras are considered by Ashwill (1983) and Smith et al. (1998) to be consistent with a middle Eocene to middle Oligocene age for the host strata. The section is capped by the ca. 30 Ma, yellow-altered, welded Tuff of Antelope Creek. This tuff is thicker and more strongly welded where it is more widely exposed in a deformed northwest tilted section along the southeastern margin of the caldera; it is everywhere absent within the arcuate ring-fracture. The younger intracaldera facies of the 29.56 Ma Tuff of Smith Rock is inset into this southeast-dipping section and forms the high ridge to the right of the prominent yellow-colored hoodoos (Fig. 6). Because the Tuff of Smith Rock is ponded against and onlaps the southeast-dipping section, structural tilt is interpreted to have occurred during caldera collapse and eruption of the tuff. Gray Butte, the high peak in the background to the east, is part of a 28.82 Ma, post-subsidence rhyolite dome complex that intrudes the Tuff of Smith Rock along the ring-fracture.

Stop 1-2. The Tuff of Smith Rock: Intracaldera Facies at Smith Rock State Park [GPS coordinates –121.1349, 44.3669]

Until recently, the age, origin, and regional stratigraphic relations of the Tuff of Smith Rock have been enigmatic, largely due to limited regional geologic mapping. Previous workers (Williams, 1957; Robinson and Stensland, 1979; Obermiller, 1987; Smith et al., 1998, Sherrod et al., 2004) considered the Tuff of Smith Rock to be an exceptionally thick tuff deposit of limited areal extent. The tuff was thought to be a conformable deposit upon the rhyolite of Gray Butte and a south-southeast–dipping section of Eocene and Oligocene strata. On the basis of K/Ar ages of uncertain quality, Obermiller (1987) interpreted the Tuff of Smith Rock as part of a middle Miocene silicic tuff cone. Smith et al. (1998) demonstrated the unit was Oligocene in age, but concurred with Obermiller (1987) that the Tuff of Smith Rock formed as a silicic tuff cone and was conformable upon the Rhyolite of Gray Butte. Results from regional detailed geologic mapping indicate that the Tuff of Smith Rock is a more widespread, relatively flat-lying, ash-flow tuff that is inset into older middle Eocene to middle Oligocene strata. Pre-caldera stratigraphy, into which the tuff is ponded, may be as young as ca. 30 Ma west of Gray Butte; basaltic andesite recovered from drill core along the inferred caldera margin near Powell Buttes has a reported K/Ar age of 30.1 ± 1.1 Ma (whole rock; Evans and Brown, 1981). Mapped contact relations also demonstrate that the Tuff of Smith Rock is not conformable upon the 28.82 Rhyolite of Gray Butte,

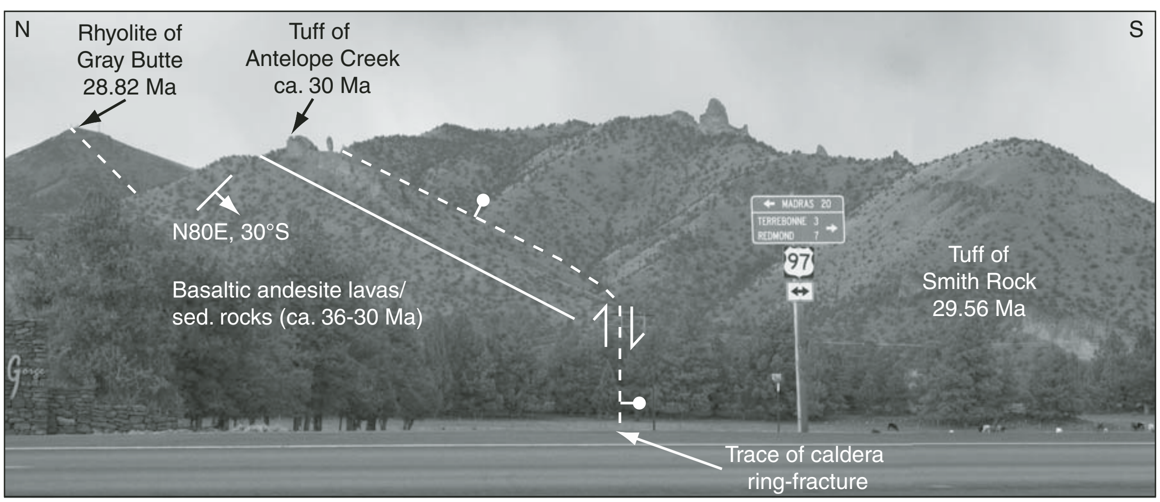

Figure 6. View east to southeast dipping section of early Oligocene strata from the old U.S 97 bridge at Peter Skene Ogden State Park at Stop 1-1. Intracaldera facies of the 29.56 Ma Tuff of Smith Rock are inset into and onlap the older deformed strata. Gray Butte in the distance is a 28.82 Ma rhyolite intrusion that crosscuts the Tuff of Smith Rock. Dashed white line demarcates the structural margin of the caldera. Arrows indicate the relative motion of the downthrown block within the caldera ring-fracture. Schematic strike and dip symbol indicates the structural orientation of early Oligocene strata.

but is instead intruded by that unit. These stratigraphic and age relations constrain the age of the intracaldera facies of the Tuff of Smith Rock between ca. 29 and 30 Ma. Smith et al. (1998) report a fission-track age of 29 ± 3.0 Ma for the intracaldera ash-flow tuff at Smith Rock State Park, and outflow facies of the tuff at McKay Saddle, Haystack Reservoir, Teller Flat, and Antelope return radiometric ages of ca. 29.6 Ma.

The intracaldera facies of the Tuff of Smith Rock forms an arcuate belt of discontinuous exposures that extends from the type section at Smith Rock State Park (Robinson and Stensland, 1979) to Ochoco Reservoir (Fig. 4). At Smith Rock State Park, the intracaldera facies weathers to spectacular spires up to 200 m tall (Fig. 7A); along the northeast margin and interior of the caldera, similar tuff deposits degrade to form rounded, low-elevation hills. The intracaldera facies is predominantly a massive, unstratified, matrix-supported, pumice-rich, sparsely sanidine-phyric, rhyolite tuff that weathers tan to yellow brown. Locally the tuff is altered to light green and maroon and is case-hardened by zeolite alteration. Bedding features in the Tuff of Smith Rock are generally indistinct, but horizontal to gently dipping (<5°) lithic-rich lenses and associated fine-grained ash horizons are intercalated with the pumice-rich tuff in exposures along the Crooked River at Smith Rock State Park and in Skull Hollow. These discontinuous lithic-rich lenses are interpreted as lithic lag-breccias that are indicative of pulsating or surging pyroclastic flows (Fig. 7B). Rare clasts of limestone, some bearing Permian fusulinids (Thompson and Wheeler, 1942), occur as xenoliths within the tuff, suggesting that the Tuff of Smith Rock erupted through a Paleozoic limestone basement. Geochemical samples analyzed from the intracaldera facies of the Tuff of Smith Rock closely compare to those determined for rhyolite dome complexes, which intrude the tuff along the margin and in central areas of the caldera (Fig. 7A; Table 1).

The intracaldera ash-flow tuff is typically in complex, high-angle to vertical contact with country rock, and water-well logs within the caldera indicate that the tuff thickens to hundreds of meters immediately away from these contacts. On the basis of regional mapping and water well log analysis of the intracaldera facies, the Tuff of Smith Rock has a minimum intracaldera thickness of 0.5 km. Bulk volume estimates of the intracaldera facies indicate more than 580 km^3 of tuff were erupted during caldera formation. This is a minimum estimate as it does not account for correlative outflow tuff deposits exposed outside the caldera ring fault. Outflow facies are exposed discontinuously around the periphery of the caldera, distributed in three geographic lobes at Haystack Reservoir, McKay Saddle, and Prineville Reservoir (Fig. 4). Distal welded ash-flow tuff deposits, up to 5 m thick, have been traced as far north as Antelope, 58 km northeast of Smith Rock (Fig. 1; Table 1).

Stop 1-3. Rhyolite of Grizzly Mountain: Post-Collapse Ring-Fracture Rhyolite Domes [GPS coordinates –120.9578, 44.4317]

Grizzly Mountain, a post-caldera rhyolite dome and flow field along the northeast margin of the Crooked River caldera, is the highest standing point of the caldera at 1733 m. The lower summit location of Stop 1-3 affords one of central Oregon's most scenic and relatively unknown vistas (Fig. 8). Rhyolite dome complexes are commonly associated with calderas after their formation and are often emplaced close to or above caldera-bounding faults (e.g., Smith and Bailey, 1968; Lipman, 1984; Christiansen, 2001). Other domes may occur aligned along regional structural trends or scattered randomly within the caldera (Lipman, 1984; Self et al., 1986). Following collapse of the Crooked River caldera, large (20–80 km^2) fields of rhyolite flows, domes, and dikes, geochemically similar to the Tuff of Smith Rock, were emplaced along the structural margin of the caldera and intruded central portions of the intracaldera ash-flow tuff (Fig. 7A; Table 1). These include the rhyolite domes and flows at

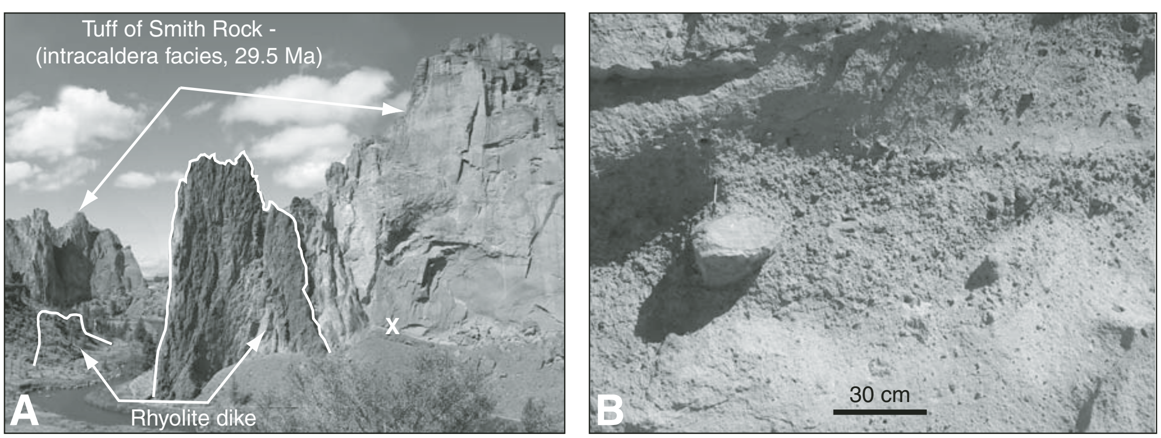

Figure 7. (A) Exposure of the intracaldera facies of the Tuff of Smith Rock at Smith Rock State Park (Stop 1-2), where it is intruded by numerous rhyolite dikes. The X in the lower right corner of A shows the outcrop location of B. (B) Lithic-rich intracaldera tuff at Smith Rock State Park.

Grizzly Mountain as well as other domes and flows at Gray Butte (265°), Powell Buttes (180°), Barnes Butte (135°), and Ochoco Reservoir (120°) (Figs. 4 and 8). Satellite rhyolite domes form Juniper Butte (285°) and Pilot Butte (125°, in the far distance) outside the northwest and southeast caldera margins, respectively. Radiometric ages of the rhyolite dome complexes range from ca. 28.8 Ma to 25.8 Ma; no rhyolites have yet been identified that were emplaced prior to caldera formation. Elongation of rhyolite dikes and dome complexes parallel to the caldera margin and their coincidence with an isostatic gravity low bounding the intracaldera tuff suggests the rhyolites were largely erupted from ring-fracture fault fissures. All rhyolites were apparently emplaced within the boundaries of syncollapse structural deformation, defined by the peripheral circumferential fault zone preserved in the surrounding country rock (Fig. 4).

The arcuate ring-fractures of the caldera that allowed emplacement of rhyolite intrusions also served as conduits for upward movement of hot fluids after the main subsidence phase of the caldera had ended. Many of the rhyolite dome fields are associated with hydrothermal alteration and hot spring style mercury mineralization; the rhyolite domes have been sites of past mineral exploration and limited resource production. Most notably, Barnes Butte was the site of a ca. 1940s mercury mine developed in heavily silicified rhyolite (Brooks, 1963). Powell Buttes was variably explored as a potential uranium target in the 1940s and 1950s, and geothermal potential was explored there in the 1980s (Brown et al., 1980). Isochron ages of pre-caldera basalt samples taken from hydrothermal alteration zones range from ca. 29 to 25 Ma, suggesting the timing of alteration (Smith et al., 1998). Numerous other locations along the ring fracture of the caldera also show evidence of quartz and calcite veining, hydrothermal explosion breccias, siliceous sinter, and well-laminated, silicified mudstone. Thormahlen (1984) and Gray and Baxter (1986) found detectable amounts of gold, silver, and arsenic in these deposits. The character and spatial association of these deposits within and peripheral to the caldera are consistent with deposition in geyser fields (e.g., modern Yellowstone caldera). Today, elevated temperature wells (21–43 °C) continue to be drilled in the Prineville area. These relatively warm-water wells are generally confined within or along the inferred caldera margin, although their modern heat source is unknown.

Stop 1-4. Pre-Caldera Volcanic Stratigraphy at Prineville Reservoir County Boat Ramp [GPS coordinates –120.7487, 44.1330].

The northwest tilted section exposed at the County boat ramp consists of a pre-caldera succession of rhyolite tuffs, interbedded tholeiitic basaltic andesite lavas, and volcaniclastic sedimentary rocks that lie along the southeast caldera margin (Fig. 9). Two early to middle Oligocene ash-flow tuffs, visible from the boat ramp, are part of the "southern facies" of the John Day Formation of Robinson and Brem (1981) (Fig. 1). Although these ash-flow tuffs are compositionally similar to tuffs erupted from the Crooked River caldera, they are older and erupted from vents that are yet unknown (Table 1). The lower part of the section is formed by the Tuff of Eagle Rock, a strongly welded, sparsely feldspar-phyric, locally rheomorphic pumice-lithic tuff that is up to 50 m thick along the banks of the reservoir. Robinson et al. (1990) reports a K/Ar age of 32.1 ± 0.7 Ma (plagioclase) for this tuff near Eagle Rock, 10 km northeast of the boat ramp. The younger Tuff of Antelope Creek is a sparsely sanidine-phyric, devitrified, strongly welded and locally rheomorphic ash-flow tuff, that is up to 30 m thick. The Tuff of Antelope Creek is geochemically similar to a thick crystal- and micro pumice-rich fallout tuff exposed beneath Carroll Rim in the Painted Hills for which Retallack et al. (2000) report a single crystal $^{40}Ar/^{39}Ar$ age of 29.75 ± 0.02 Ma (Tables 1 and 3).

Lavas interbedded with the ash-flow tuffs near the boat ramp mark the transition in the Lower Crooked Basin between the older

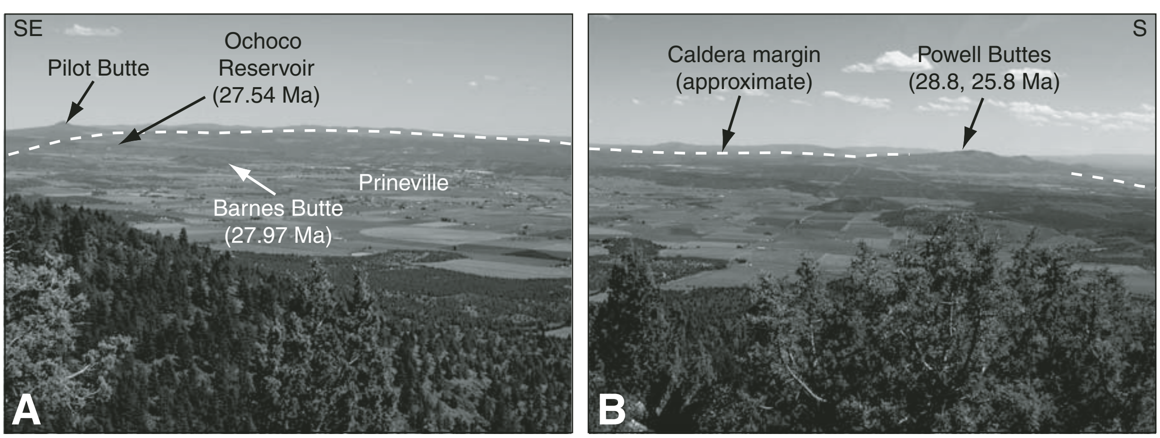

Figure 8. Panoramic view, looking south across the Crooked River caldera, from Grizzly Mountain at Stop 1-3. Rhyolite domes described in the text are labeled. Total distance of view across A and B is ~25 mi. (A) View to the southeast. (B) View to the south. Dashed white line shows the approximate location of the caldera margin.

Eocene calc-alkaline volcanism of the Ochoco volcanic field and the younger bimodal basalt and rhyolite volcanism associated with the Crooked River caldera (Fig. 5A). These lavas consist of both mafic and intermediate flows that are exposed along both the northwest and southeast margins of the caldera (Fig. 4). Intermediate composition rocks consist of tholeiitic basaltic andesite and andesite lavas, with chemical compositions similar to that of icelandite (Table 1). Petrographic and chemical characteristics of the intermediate flows indicate compositions similar to those reported by Robinson and Brem (1981) and Robinson et al. (1990) for trachyandesites in member B of the John Day Formation. Intermediate lavas are compositionally similar to a 30.8 ± 0.5 Ma intrusion (K/Ar, whole rock; Robinson et al., 1990) exposed along the northwest margin of the caldera north of Gray Butte and a 30.1 ± 1.1 Ma basaltic andesite lava flow (K/Ar, whole rocks, Evans and Brown, 1981) encountered in a geothermal test well that was drilled just west of Powell Buttes (Brown et al., 1980). The intermediate lavas are interbedded with a poorly exposed series of more mafic aphyric to sparsely olivine-phyric basalts north and west of Gray Butte (Table 1). Similar composition basalt lavas have not been found at Prineville Reservoir. Geochemical analyses of basalts indicate compositions similar to those reported by Robinson (1969), Robinson and Brem (1981), and Robinson et al. (1990) for alkali olivine basalt flows found in Members E, F, and G north of the Lower Crooked volcanic field (Table 1).

The stratigraphic section exposed at the boat ramp lies within the Prineville Reservoir fault zone, a northeast trending structural zone on the southeastern margin of the caldera (Fig. 4). The main zone of deformation is ~7 km wide by 16 km long and defines a northeast-trending homocline pervasively cut by faults with both normal and reverse sense of displacement. Beds within the homocline generally strike N45°E and dip 45°–55° northwest back into the caldera (Figs. 4 and 9). Outflow facies of the Tuff of Smith Rock overly the deformed Oligocene section, separated by an angular unconformity. East of Prineville Reservoir, along O'Neil Creek the outflow tuff is ponded against the tilted structural block and is itself faulted and warped with a northwest verging dip. The Tuff of Smith Rock is the youngest unit deformed in the fault zone. Combined stratigraphic and structural relations within the Prineville Reservoir fault zone suggest that deformation of the Oligocene section of tuff and basaltic andesite occurred synchronously with formation of the Crooked River caldera and deposition of outflow facies of the Tuff of Smith Rock.

DAY 2. THE WILDCAT MOUNTAIN CALDERA

The first half of Day 2 will traverse part of Wildcat Mountain caldera, a middle Eocene volcanic center situated in the Ochoco Mountains directly adjacent to the large ca. 10 m.y. younger Crooked River caldera. For the second part of Day 2, we will travel east to the John Day Fossil Beds National Monument where Paleogene tuffs form prominent marker beds within well-exposed stratigraphic sections (Fig. 2).

Eruption of the Tuff of Steins Pillar between 41.50 and 39.35 Ma resulted in the formation of the Wildcat Mountain caldera, located 10 km northeast of the city of Prineville in the Ochoco Mountains of north-central Oregon (Figs. 4 and 10). Post-volcanic erosion has stripped away most of the intracaldera fill and outflow deposits, and part of the original topographic rim of the caldera, leaving a distinct depression with more than 800 m of vertical relief. The caldera is drained by the tributaries and main stem of Mill Creek.

The Wildcat Mountain caldera is the major vent feature of the Ochoco volcanic field, a calc-alkaline, intermediate-to-silicic igneous system that developed along the southwestern axis of the Blue Mountains during the middle Eocene (Fig. 1). Intermediate to silicic basement rocks and rocks associated with the Wildcat Mountain caldera are characterized by relatively enriched

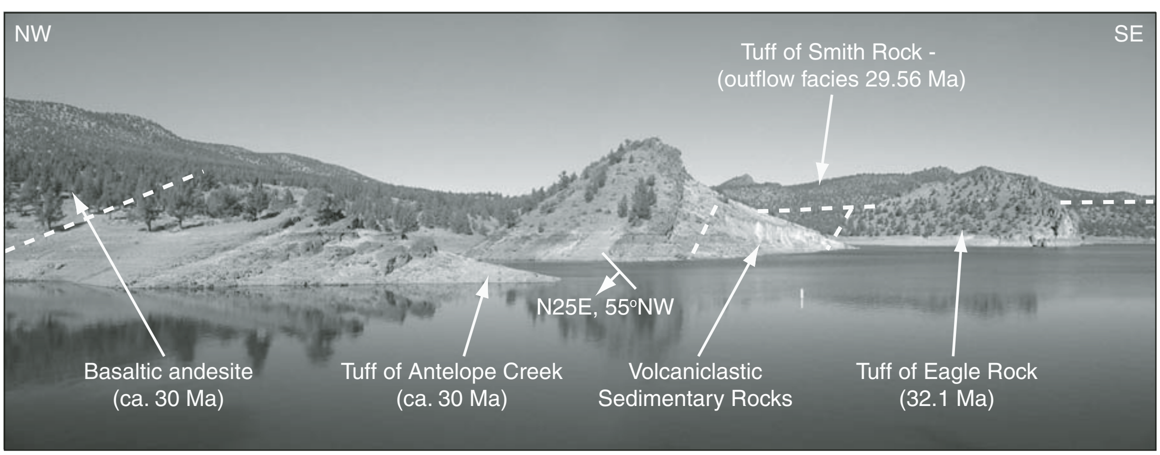

Figure 9. Northwest-dipping early Oligocene strata exposed near the Prineville Reservoir county boat ramp at Stop 1-4. The exposed section includes two thick rhyolite tuffs interbedded with Fe- and Ti-rich basaltic andesite and volcaniclastic sedimentary rocks. Dashed white lines are approximate contacts between units. Schematic strike and dip symbol indicates the structural orientation of early Oligocene strata.

amounts of Al_2O_3 and corresponding relatively depleted contents of FeO*. These rocks display characteristically low contents of incompatible high-field strength elements such as Nb and Zr, low contents of Y, and generally have lower abundances of the light rare earth elements La and Ce (Fig. 5; Table 2). The earliest recognized magmatism associated with the Ochoco volcanic field produced a series of variably eroded, overlapping andesite and dacite lavas, domes, and shallow intrusions at 43.86 ± 0.89 Ma ($^{40}Ar/^{39}Ar$, plagioclase; Ferns and McClaughry, 2007). Massive andesite lavas erupted around the northern margin of the volcanic center at 41.50 ± 0.48 Ma ($^{40}Ar/^{39}Ar$, plagioclase), although no evidence of any volcanic edifice preceding caldera formation has been found. Initial intermediate volcanism in the field was followed closely by eruption of the Tuff of Steins Pillar between 41.50 and 39.35 Ma and synvolcanic subsidence of a 16 × 11 km volcano-tectonic depression that defines the Wildcat Mountain caldera. Rhyolite and dacite lavas, domes, and intrusions were emplaced along the ring-fracture and in central vent areas around 39.35 ± 0.30 Ma ($^{40}Ar/^{39}Ar$, plagioclase) following the main subsidence phase. Repeated injection of silicic magma within central areas of the caldera formed a prominent central resurgent dome that was accompanied by the emplacement of linear breccia pipes and hydrothermal alteration along the ring-fracture. This phase of magmatic and hydrothermal activity around the periphery of the Wildcat Mountain caldera produced the mercury mineralization between Kidnap Springs and Strickland Butte that was explored by prospectors, and to a limited extent mined between 1940 and 1942 (Brooks, 1963). Post-mineralization emplacement of

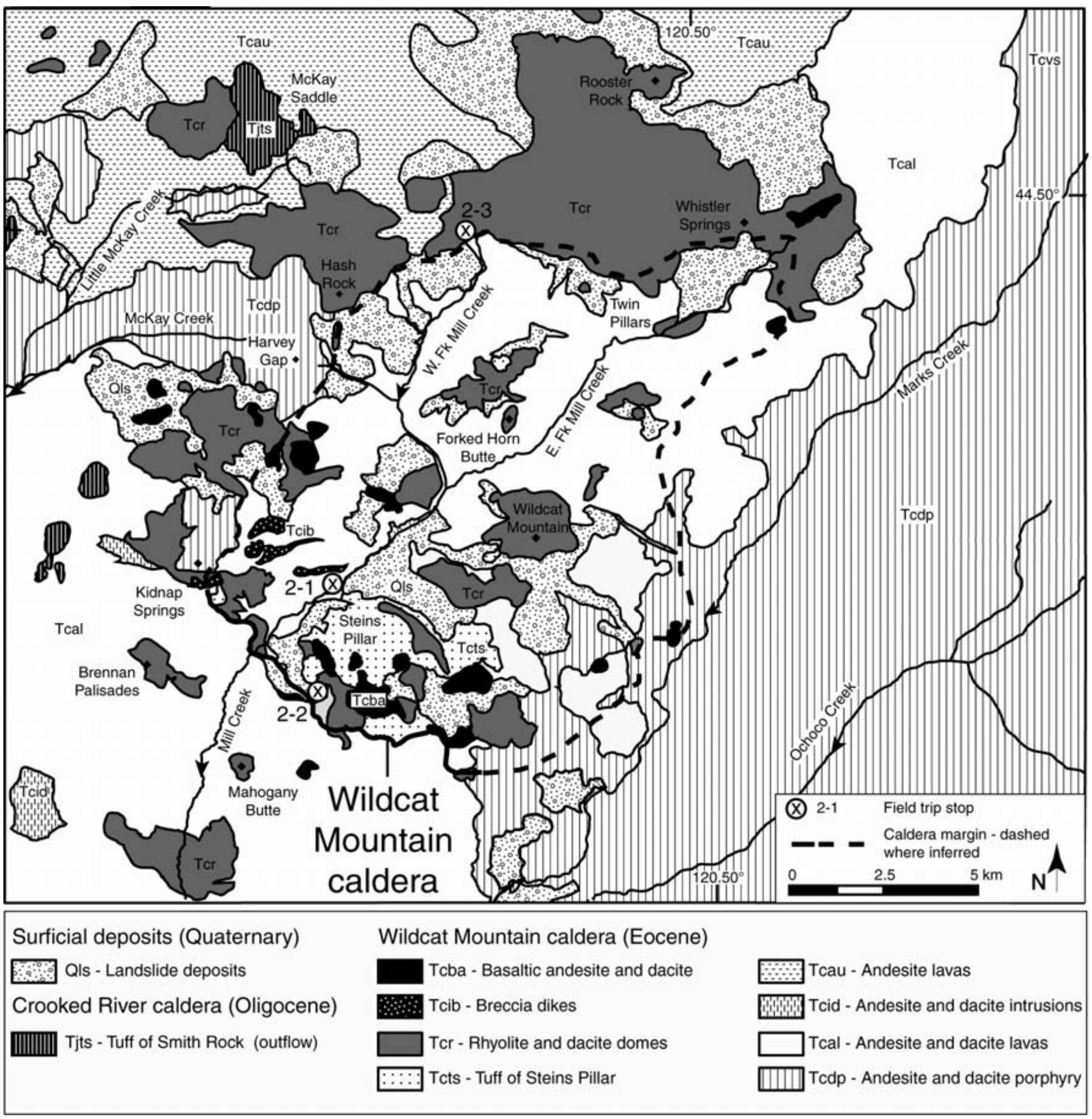

Figure 10. Simplified geologic map of the Wildcat Mountain caldera labeled with associated field stops.

TABLE 2: WHOLE-ROCK ANALYSES OF SELECTED ROCKS FROM THE OCHOCO VOLCANIC FIELD AND WILDCAT MOUNTAIN CALDERA

	Pre-caldera intermediate rocks					Tuff of Steins Pillar	Post-caldera rhyolite			Post-caldera dacite		Post-caldera intermediate rocks	
Sample number:	279 LCJ 06	45 P 05	59 LC 06	89 LCJ 06	119 LCJ 06	151 LCJ 07	149 LC 06	280 LCJ 06	269 LCJ 06	125 LCJ 06	101 LCJ 06	360 LCJ 07	423 LCJ 07
Geographic area:	Harvey Gap	Mill Creek	Old Dry Creek	School-house Creek	Jesse Spring	Steins Pillar	Wildcat Mt.	Hash Rock	Twin Pillars	Forked Horn Butte	Green Mt.	Salmon Creek	Sears Creek
UTM N:	4926670	4915308	4918300	4919486	4929665	4919034	4922150	4929440	4928305	4925964	4923605	4918279	4919601
UTM E:	688690	685994	682290	687237	692047	688149	695180	694450	695980	694194	685502	692456	698232
Age (Ma):	43.86	42.79			41.50			39.35	39.35				
SiO_2	58.21	65.76	59.42	62.51	57.12	75.08	76.11	74.68	73.96	67.91	68.66	55.78	61.45
Al_2O_3	17.83	15.60	15.89	17.16	16.40	13.53	13.25	13.75	13.81	16.11	16.13	16.49	16.36
TiO_2	0.82	0.68	1.13	0.82	1.47	0.23	0.13	0.20	0.30	0.61	0.54	1.17	0.91
FeO*	6.58	4.94	8.42	5.64	8.96	2.19	1.96	2.21	2.11	4.52	3.62	9.02	6.17
MnO	0.11	0.07	0.17	0.11	0.21	0.02	0.02	0.02	0.04	0.17	0.06	0.14	0.11
CaO	7.64	4.87	6.47	5.94	7.41	2.87	0.40	0.94	1.29	3.83	3.53	8.07	6.18
MgO	4.02	2.18	3.17	2.39	3.45	1.00	0.00	0.00	0.11	0.56	0.72	4.67	3.68
K_2O	1.32	2.19	1.51	1.42	1.37	4.31	5.16	3.90	3.91	2.12	2.12	1.10	1.71
Na_2O	3.28	3.52	3.41	3.80	3.35	0.72	2.92	4.27	4.39	3.98	4.47	3.23	3.18
P_2O_5	0.18	0.18	0.42	0.21	0.27	0.04	0.04	0.03	0.07	0.20	0.14	0.33	0.24
LOI	1.59	2.57	1.84	1.71	1.24	8.68	1.65	1.16	1.13	3.41	2.02	2.12	3.02
Ni	73	20	43	15	26	3	1	2	1	20	10	48	21
Cr	91	39	49	27	46	13	1	0	2	33	14	70	64
Sc	20	13	20	16	25	7	3	6	5	11	11	22	15
V	136	89	145	122	207	26	12	9	16	71	52	201	134
Ba	341	528	450	521	346	657	1010	950	935	512	715	261	445
Rb	43.8	86.7	37.9	39.6	53.0	125.9	184.5	128.7	139.2	62.2	60.6	30.4	67.8
Sr	383	357	347	406	346	289	31	88	93	302	370	434	393
Zr	148	153	269	187	164	111	158	299	266	233	202	215	182
Y	20.8	14.4	31.1	21.6	29.1	19.0	34.2	26.6	24.2	24.0	23.3	27.3	23.1
Nb	9.2	9.6	20.3	10.8	12.5	13.3	12.2	16.7	14.4	14.1	11.3	15.7	12.2
Ga	17.4	18.1	18.8	17.6	18.7	12.6	16.1	16.1	17.2	17.4	16.7	20.4	17.7
Cu	54	28	63	36	54	5	2	1	5	27	27	112	33
Zn	66	55	94	67	88	35	52	51	44	69	53	94	76
Pb	4	4	6	7	5	6	9	10	10	9	9	3	4
La	16	21	25	21	16	23	42	37	35	31	26	19	21
Ce	31	47	52	38	34	40	79	75	71	55	54	40	43
Th	4.9	5.8	3.8	4.0	3.9	13.6	4.4	14.8	16.1	4.7	6.0	4.3	3.9
U	0.7	1.9	0.8	1.9	1.8	3.0	0.0	3.7	4.5	3.1	1.6	0.0	1.2
Co	23	12	24	17	29	0	0	0	0	10	5	28	13

Note: Major element determinations have been normalized to a 100% total on a volatile-free basis and recalculated with total iron expressed as FeO*. Oxides as weight percent; trace elements as parts per million.

basaltic andesite to andesite lavas and plugs occurred along caldera margin until ca. 38–36 Ma, when major volcanic activity in the field ceased.

Intermediate composition rocks of the Ochoco volcanic field that preceded formation of the Wildcat Mountain caldera are equivalent to rocks of the upper Clarno Formation that record a regionally widespread magmatic pulse between ca. 44 and 41 Ma (Waters et al., 1951; Swanson and Robinson, 1968; Swanson, 1969; Enlows and Parker, 1972; Walker and Robinson, 1990; Appel, 2001; Bestland et al., 1999). The Tuff of Steins Pillar and post-collapse rhyolites erupted from the Wildcat Mountain caldera between 41.50 and 39.35 Ma are temporally correlative to member A (39.2–39.7 Ma) of the John Day Formation. Rocks of the middle Eocene Wildcat Mountain caldera therefore overlap the inferred transition between the Clarno and John Day Formations, and record the onset of Paleogene ash-flow tuff eruptions in north-central Oregon (Fig. 3).

Stop 2-1. Steins Pillar Viewpoint [GPS coordinates –120.6176, 44.4173]

Steins Pillar and Wildcat Mountain are two of the most prominent features in the Wildcat Mountain caldera (Figs. 11A and 11B). Steins Pillar is one of a series of north-northwest trending spires of strongly welded intracaldera tuff (Fig 11B). The pillar is ~106 m tall and consists of a compound cooling unit of pink to buff colored, massive to flow-banded, variably spherulitic, lithophysal, rheomorphic tuff. The tuff is propylitically altered with secondary quartz and small calcite veins; thin breccia veins are locally pervasive. Wildcat Mountain, visible on the east-northeast (80°), is part of a post-caldera rhyolite dome complex that intrudes the Tuff of Steins Pillar (Fig 11A). White-colored outcrops exposed below the summit are part of the intracaldera tuff.

Waters (1966) first described Steins Pillar as an "accumulation of hot pumice fragments, glass shards, and violently vesiculating lava that frothed from numerous volcanic orifices, many of whose sites are now filled with plugs, domes, and dikes of rhyolite. Among these former centers of eruption are the ridges on either side of Benefield Creek, Forked Horn Butte, Mahogany Butte, and many unnamed sharp buttes both to the north and south of Stein's Pillar (Fig. 10). The flows of hot pumice fragments and glass shards pouring from these volcanic centers spread into and filled an ancient broad valley. Part of the valley, in the area between Wildcat Mountain and Stein's Pillar, now lies buried beneath as much as 1000 feet of sintered and welded tuff."

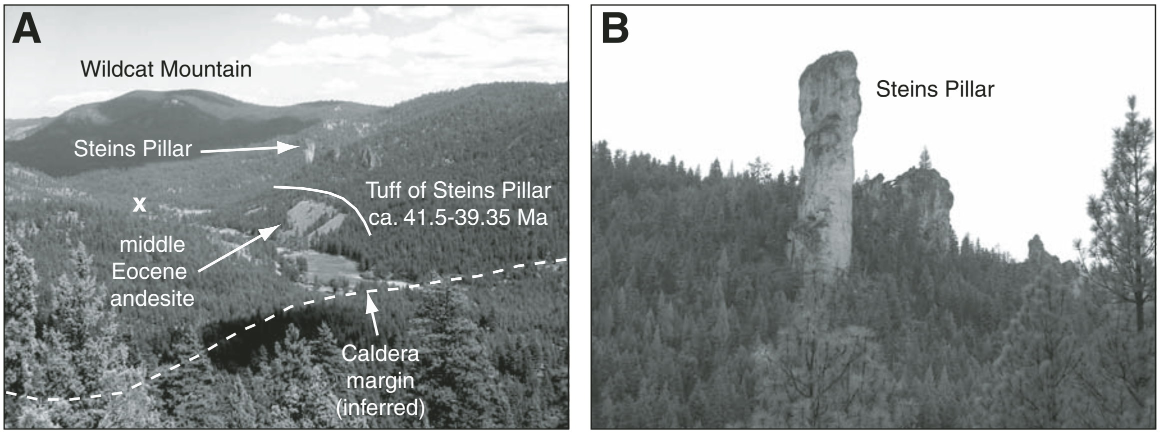

Figure 11. (A) View of the southwest margin of the Wildcat Mountain caldera, showing the location of Wildcat Mountain and Steins Pillar. Dashed white line shows the approximate location of the caldera margin. The X in the center-left of the photograph shows the location of Stop 2-1. (B) Steins Pillar as viewed from the parking area at Stop 2-1.

The Tuff of Steins Pillar is now interpreted as the eruptive product of a single cataclysmic eruption in the middle Eocene that formed the Wildcat Mountain caldera.

Stop 2-2. The Tuff of Steins Pillar and Post-Subsidence Rhyolite Dikes [GPS coordinates –120.6216, 44.3932]

The rheomorphic intracaldera tuff exposed at Steins Pillar, is succeeded upward by at least 305 m of massive, poorly sorted, non-welded to weakly welded, locally propylitically altered and zeolitized, lithic- and pumice-rich tuff (Fig. 12). Diffuse layering in the tuff is defined by alternating layers of lithics and pumices. Lithics consist of aphyric to vesicular andesite rock fragments and flow-banded, aphyric rhyolite. Andesite lithics are composed of an equigranular plagioclase and pyroxene groundmass, are angular, and have a maximum size of 10 cm across; these clasts average 2–5 cm across. Rhyolite lithics are spherulitic, flow banded, angular, and reach a maximum size of 37 cm across; rhyolite clasts average 10–15 cm across. Pumices are white to pale-green, banded, average 2–4 cm in length, are moderately flattened, and are generally aligned in outcrop. Lithics and pumices are encased in a matrix of sparsely scattered, anhedral, clear to white sanidine crystals, sparse hornblende needles, and devitrified glass and ash. The tuff contains characteristically low contents of Nb (12.4–13.8 ppm), Zr (110–145 ppm), Y (19–27.9 ppm), La (23–29 ppm), and Ce (40–58 ppm) (Table 2).

Outflow facies of the Tuff of Steins Pillar are completely absent in the vicinity of Wildcat Mountain caldera and have not been yet been identified elsewhere in the region. Stratigraphic position of the Tuff of Steins Pillar above 41.50 ± 0.48 Ma andesite lavas and beneath the 39.35 ± 0.30 Ma Rhyolite of Hash Rock on the north rim of the caldera indicates this unit is approximately temporally correlative but slightly older than the widespread 39.2–39.7 Ma Member A tuff, which regionally defines the base

Figure 12. Pumice-lithic tuff that forms part of the intracaldera facies of the Tuff of Steins Pillar at Stop 2-2. The scale in the lower part of the photograph is 16 cm long.

of the John Day Formation (Fig. 3; Peck, 1964; Swanson and Robinson, 1968; Robinson, 1975, Robinson et al., 1990; Smith et al., 1998; Retallack et al., 2000). Member A has similar chemical affinities as the Tuff of Steins Pillar, but is distinguished on the basis of its relatively elevated amounts of incompatible high field strength elements such as Nb (27.3–34.8 ppm) and Zr (219–339 ppm), higher contents of Y (69–90 ppm), and higher contents of the light rare earth elements, La (43–81 ppm) and Ce (121–124 ppm) (P.E. Hammond, 2008, personal commun.).

Stop 2-3. The Rhyolite of Hash Rock and Twin Pillars Viewpoint [GPS coordinates –120.5723, 44.4955]

The Rhyolite of Hash Rock, part of a post-caldera lava field, is visible at Stop 2-3, along with a panoramic view from north to south across the Wildcat Mountain caldera (Fig. 13). The Rhyolite of Hash Rock forms a nearly continuous rim and plateau around the northern margin of the Wildcat Mountain caldera. The rhyolite is purple-gray, aphyric to sparsely plagioclase-phyric, with euhedral plagioclase laths up to 3 mm long. Outcrops typically are distinctly flow banded with tight flow-folds. A fresh glassy vitrophyre and dense lithophysal zones are locally common along the margins and at the base of the lava. The lava, erupted from fissure-conduits now preserved south of Hash Rock and at Twin Pillars (65°), covers an area of ~50 km^2 extending outward from the caldera to Rooster Rock (Fig. 10; Table 2). The lava ranges in thickness from 180 m near Hash Rock to over 305 m at the viewpoint west of Whistler Springs. An $^{40}Ar/^{39}Ar$ age of 39.35 ± 0.30 Ma (plagioclase) was obtained from a sample on the plateau above the east fork of Mill Creek where the rhyolite overlies bedded airfall deposits related to the climatic eruption of the Tuff of Steins Pillar.

The interior of the caldera, visible in the middle-ground east of the viewpoint is marked by a prominent northeast elongated, ~11 km^2 (7 mi^2) rectilinear ridge that forms the drainage divide between the east and west forks of Mill Creek (Figs. 10 and 13). The ridge is a resurgent dome formed by the repeated injection of silicic magma into central parts of the caldera following the main subsidence phase. The resurgent dome parallels the major long axis of the caldera and is composed of andesite basement rock intruded by numerous dacite and rhyolite dikes and plugs. Forked Horn Butte, visible on the southeast (90°) is one of the high-standing rhyolite plugs.

Following collapse of the Wildcat Mountain caldera rhyolite lavas, domes, plugs and dikes, geochemically similar to the Tuff of Steins Pillar, were emplaced along the structural margin of the caldera and intruded central portions of the intracaldera ash-flow tuff (Table 2). These include rhyolites that form Hash Rock and Twin Pillars, as well as Strickland Butte, Forked Horn Butte, Wildcat Mountain, Brennan Palisades, Mahogany Butte, and numerous other less prominent ridges and buttes in and around Wildcat Mountain caldera (Fig. 10). Most of the rhyolites either intrude or overlie the intracaldera facies of the tuff of Steins Pillar; no rhyolites have yet been identified that were definitively emplaced prior to caldera formation. Elongation of some rhyolite dikes and domes parallel to the caldera margin suggests that these complexes were likely erupted from ring-fracture fissures. Other rhyolite intrusions and dikes are elongated in a northwest-southeast direction parallel to the predominant structural fabric observed in local faults and pre-caldera intermediate dikes.

The arcuate ring-fractures of the caldera and local northwest-southeast oriented fault structures that allowed emplacement of rhyolite intrusions also served as conduits for upward movement of hot fluids after the main subsidence phase

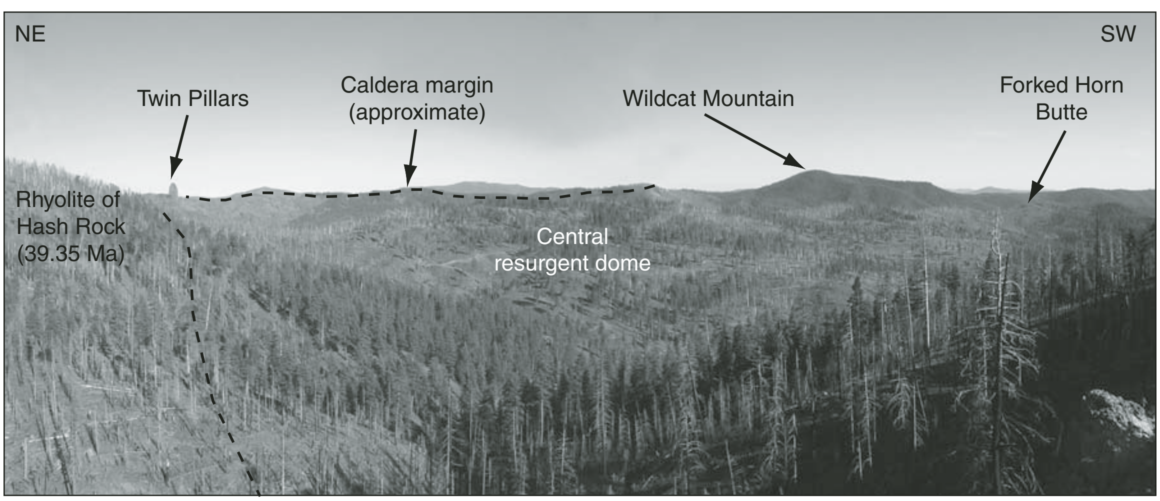

Figure 13. Panoramic view across the Wildcat Mountain caldera from Stop 2-3. The Rhyolite of Hash Rock forms the plateau around the north part of the caldera. The remnant feeder conduit for this flow is exposed at Twin Pillars, visible in the distance to the east. Wildcat Mountain, a post-subsidence rhyolite dome is visible to the southwest. The central part of the caldera is formed from a central resurgent dome that is marked by a series of post-subsidence intrusions such as the rhyolite plug at Forked Horn Butte. Dashed black line shows the approximate trace of the caldera margin.

of the caldera had ended. The rhyolite dome complex at Strickland Butte along the western margin of the caldera is associated with hydrothermal alteration and fracture-coating mercury mineralization; this area was a site of past mineral exploration and limited resource production. Most notably, the area between Kidnap Springs and Strickland Butte was the site of ca. 1940s mercury mine developed in silicified rhyolite (Brooks, 1963). Numerous other locations along the ring fracture of the caldera also show evidence of mercury mineralization and agate-filled geodes are locally abundant, associated with lithophysal zones within rhyolite lavas and intrusions.

John Day Fossil Beds National Monument

The Turtle Cove Member, exposed in the Painted Hills and Sheep Rock Units of the John Day Fossil Beds National Monument, is the thickest and most regionally extensive member in the "eastern" facies of the John Day Formation (Fig. 3; Fisher and Rensberger, 1972; Robinson et al., 1984; Bestland, 1995). This part of the John Day Formation, ranging in age from ca. 30.4 to 22.6 Ma, is famous for its picturesque blue-green tuffs, spectacular pinnacled peaks, and rich fossil record (Fig. 3) (Bestland, 1995). Prominent tuff marker beds that punctuate the fossil-bearing sedimentary sections have provided an important time-datum that has allowed for the detailed characterization of one of the richest fossil records of Tertiary plants and animals in North America. New geochemical data, augmented by high-precision $^{40}Ar/^{39}Ar$ geochronology, now allows tentative regional correlation of tuffs preserved within the John Day Fossil Beds National Monument with corresponding source calderas.

Stop 2-4. Painted Hills Unit: Carroll Rim Trail and Viewpoint [GPS coordinates –120.2662, 44.6522]

The Turtle Cove Member exposed beneath Carroll Rim in the Painted Hills consists of a succession of paleosols, punctuated by at least three distinct tuff marker beds (Fig. 14). The two lowest exposed tuffs are white, massive, devitrified, crystal-pumice airfall units that have concordant single crystal $^{40}Ar/^{39}Ar$ ages of 29.75 ± 0.02 (lower sanidine tuff) and 28.70 ± 0.06 Ma (upper white tuff) (Bestland and Retallack, 1994b; Retallack et al., 2000). Geochemical analyses for these tuffs are reported in Table 3. The lower sanidine tuff is temporally equivalent with the Crooked River caldera, but it is chemically distinct from outflow sheets of the 29.56 Ma Tuff of Smith Rock (Tables 1 and 3). This tuff arguably shares similar geochemical traits with the stratigraphically correlative Tuff of Antelope Creek, which sits directly beneath outflow facies of the Tuff of Smith Rock along the northwest and southeast margins of the Crooked River caldera (Tables 1 and 3).

Member H (Robinson et al., 1984; "Picture Gorge ignimbrite" of Fisher, 1966), which caps Carroll Rim, is a compound pyroclastic flow unit characterized by a locally brecciated basal

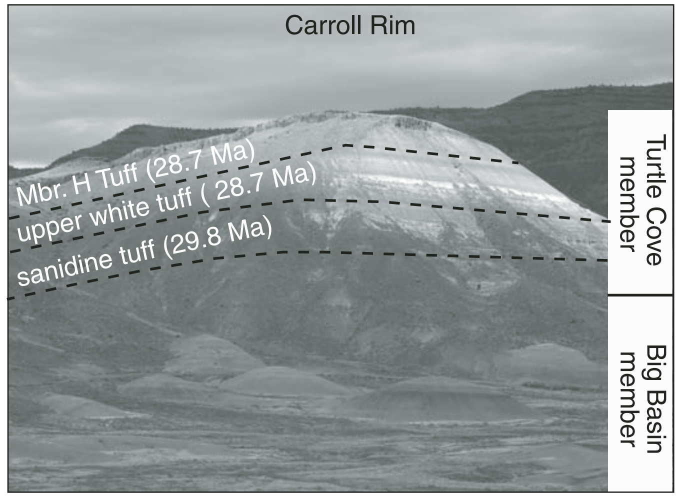

Figure 14. The Turtle Cove Member exposed at Carroll Rim in the Painted Hills Unit of the John Day Fossil Beds National Monument. View is to the northeast from the Carroll Rim trailhead. Dashed black lines mark the approximate contacts between tuff units.

TABLE 3. WHOLE-ROCK GEOCHEMICAL ANALYSES OF TUFFS IN THE JOHN DAY FOSSIL BEDS NATIONAL MONUMENT

	Lower sanidine tuff	Upper white tuff	Member H: Vitrophyre–lower cooling unit		Member H: Main flow–upper cooling unit	
Sample no.:	PAT PHR3	PAT PHR2	†CCR-JD1A	†CCR-F1C	PAT PHR1	JD-FR-1
Geographic area:	Carroll Rim	Carroll Rim	Carroll Rim	Foree	Carroll Rim	Foree
UTM N:	4947971	4948075	4948170	4947484	4948170	4947484
UTM E:	716890	716967	716890	291050	716890	291050
Age (Ma):	29.75	28.70	28.65		28.65	
SiO_2	76.54	74.46	74.90	75.90	82.32	81.06
Al_2O_3	12.42	13.45	12.85	12.50	9.5	8.71
TiO_2	0.35	0.35	0.23	0.21	0.18	0.28
FeO*	2.73	2.55	2.89	2.36	0.48	2.64
MnO	0.04	0.02	0.06	0.08	0.04	0.03
CaO	1.76	1.79	0.90	0.84	0.44	0.81
MgO	0.59	0.42	0.39	0.06	0.03	0.46
K_2O	3.41	3.7	4.85	3.38	4.38	3.37
Na_2O	2.13	3.21	2.89	4.66	2.61	2.55
P_2O_5	0.03	0.06	0.03	0.02	0.04	0.08
LOI	11.39	13.25	**N.D.	**N.D.	2.00	2.51
Ni	0.0	0.0	0.0	0.0	0.2	0.0
Cr	8.3	3.1	3.5	1.8	2.4	0.0
Sc	5.3	5.8	2.9	2.7	2.3	6.0
V	24.6	16.1	6.2	2.3	11.0	36.0
Ba	669.5	1569.6	808.8	875.8	677.4	575.0
Rb	60.2	69.6	128.6	111.5	88.2	86.5
Sr	271.2	369.3	48.2	34.7	29.0	52.0
Zr	435.2	340.3	487.4	473.8	374.3	344.0
Y	49.1	35.2	100.8	105.1	74.8	67.7
Nb	35.5	28.2	59.6	60.5	45.7	41.4
Ga	23.3	20.8	25.3	25.5	19.8	18.2
Cu	10.1	6.2	2.8	3.0	1.3	0.0
Zn	127.9	113.1	149.1	150.8	30.2	90.0
Pb	14.7	13.4	10.8	12.7	9.9	5.0
La	41.7	34.9	73.9	72.6	59.1	44.0
Ce	99.7	80.8	154.1	155.6	117.8	90.0
Th	12.7	11.1	14.6	15.7	12.5	7.6
U	3.8	4.0	5.2	4.8	3.6	3.3
Co	0	0	**N.D.	**N.D.	0	0

Note: Major element determinations have been normalized to a 100% total on a volatile-free basis and recalculated with total iron expressed as FeO*. Oxides as weight percent; trace elements as parts per million. LOI—loss on ignition.

† Ricker and Streck (2009, unpublished data).

**N.D. = no data or element not analyzed.

vitrophyre and an overlying weakly to strongly welded, red-gray pumice-lithic tuff. This ash-flow tuff forms a regionally widespread unit that is an important stratigraphic marker in both the "eastern" and "western" facies of the John Day Formation. Retallack et al. (2000) report single crystal $^{40}Ar/^{39}Ar$ ages of 28.65 ± 0.05 Ma and 28.65 ± 0.07 Ma for Member H at Carroll Rim. Member H is stratigraphically equivalent to the Tuff of Barnes Butte in Prineville, which was erupted within the confines of the Crooked River caldera at ca. 28.5 Ma (McClaughry and Ferns, 2006a). Similar lithologic character, age, and geochemistry between the Member H tuff and the Tuff of Barnes Butte suggest a correlation between these units and may indicate the Crooked River caldera was the eruptive source (Tables 1 and 3). A Crooked River caldera source for Member H is consistent with the work of Fisher (1966) who indicated a probable eruptive center in the Ochoco Mountains southwest of Mitchell.

Stop 2-5. Sheep Rock Unit: Thomas Condon Paleontology Center [GPS coordinates –119.6437, 44.5531]

The Thomas Condon Paleontology Center in the Sheep Rock Unit of the John Day Fossil Beds National Monument features exhibits that showcase some of the spectacular paleontological specimens that have been recovered from the John Day Formation. A short hike up the trail that begins near the south end of the parking area ascends to an overlook of Sheep Rock and the John Day River. Sheep Rock is formed from a well-exposed section of the Turtle Cove Member, which here consists of an assemblage of blue-green to tan variably zeolitized siltstones and paleosols and interbedded tuffs (Figs. 3 and 15; Bestland, 1995). The Member H tuff forms a prominent marker bed at the midpoint of the stratigraphic section (Fisher, 1966; Bestland, 1995). Geochemical results obtained from Member H in the Foree area several miles north of Sheep Rock, are similar to analyses for the capping tuff at Carroll Rim, permitting regional chemical correlation of these distant exposures (Table 3). The section at Sheep Rock is capped by a remnant of middle Miocene Columbia River Basalt.

DAY 3. THE TOWER MOUNTAIN CALDERA

Day 3 of the field trip will focus on the Oligocene Tower Mountain caldera, the easternmost of the three known Paleogene calderas in Oregon (Figs. 1 and 2). The Tower Mountain caldera is similar in age to the Crooked River caldera, but shares a chemical affinity more closely aligned with that of the ca. 10–13 m.y. older Wildcat Mountain caldera (Fig. 5; Tables 2 and 4). Eruption of the Tuff of Dale between 29.8 and 28.1 Ma resulted in the formation of the Tower Mountain caldera, a ~15-km-wide, roughly circular volcanic center exposed 29.5 km southeast of Ukiah (Fig. 16). The caldera is defined by an arcuate belt of rhyolite intrusions that encircle a thickly ponded resurgent core of ash-flow tuff centered on Tower Mountain, for which the structure is named. The topographic high of the caldera forms the drainage divide between tributaries of the Upper Grande Ronde and North Fork of the John Day Rivers.

The Tower Mountain caldera is part of the late Oligocene bimodal basalt and rhyolite Tower Mountain volcanic field that covers an area of more than 500 km^2 in the Blue Mountains of northeast Oregon (Ferns et al., 2001). Formation of the Tower Mountain caldera was preceded by both tholeiitic alkali olivine basalts characterized by high amounts of FeO*, TiO_2, and K_2O, and high Al_2O_3, low K_2O olivine basalts and intermediate rocks of basaltic andesite to dacite compositions (Fig. 5; Table 4). Silicic rocks associated with syncollapse and post-subsidence phases of the caldera have a calc-alkaline chemical affinity. These rocks display characteristically low contents of incompatible high-field strength elements, such as Nb, and generally have lower abundances of the light rare earth elements (Fig. 5). Although Nb contents in the rhyolites are typically low, ranging between 10 and 20 ppm, some post-subsidence porphyritic rhyolite domes and intrusions at Tower Mountain contain as much as 50 ppm Nb.

Volcanism in the Tower Mountain volcanic field began at ca. 29.8 Ma, when channel-filling tholeiitic and alkalic olivine basalt lavas erupted from a vent area straddling the tectonic boundary between pre-Tertiary accreted terranes. The largely broken mélange rocks of the Baker Terrane reside on the south (Fig. 16) (Silberling et al., 1984) while chlorite and biotite schists of the Mountain Home Metamorphic Complex are situated on the north (Ferns et al., 2001). Early mafic eruptions were followed by the emplacement of debris flows and the eruption of a series of thick porphyritic dacite and andesite lavas. Subsequently, a climactic caldera-forming eruption resulted in the eruption of the Tuff of Dale and the formation of the Tower Mountain caldera. During the post-subsidence phase, a series of rhyolite domes were extruded along arcuate ring fractures along with aphyric to porphyritic dacite and rhyolite masses that intruded the intracaldera tuff, forming the resurgent core of the caldera. Silicic volcanism

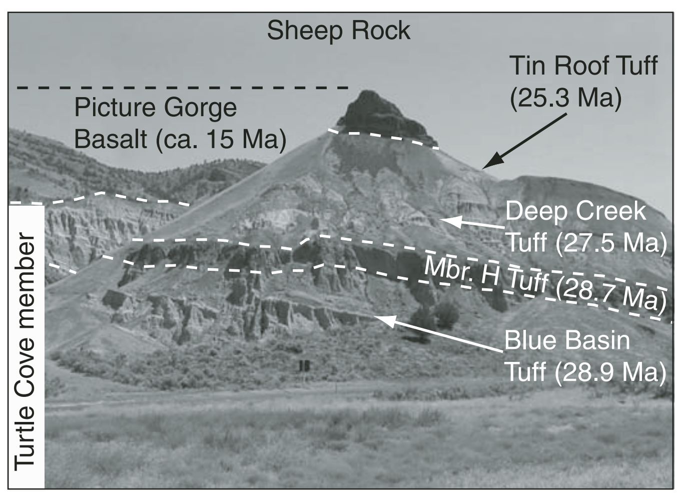

Figure 15. The Turtle Cove Member exposed at Sheep Rock in the Sheep Rock Unit of the John Day Fossil Beds National Monument. Dashed white lines mark the approximate contacts between tuff units.

TABLE 4. WHOLE-ROCK GEOCHEMICAL ANALYSES OF SELECTED ROCKS FROM THE TOWER MOUNTAIN VOLCANIC FIELD AND TOWER MOUNTAIN CALDERA

	Pre-caldera basalts, andesites, and dacites					Tuff of Dale					Post-caldera rhyolite domes, flows, and intrusions			Post-caldera andesite
						Intracaldera tuff		Outflow tuff						
Sample number:	97-LG-123	97-LG-113	AR-106	96-LG-21	96-LG-74	97-LG-78	97-LG-68	CGH31	CGH32-B pumice	97-LG-130	CGH10	CGH02B	97-LG-23	97-LG-130
Geographic area:	Tower Mt.	Tower Mt.	Rocky Point	Sheep Creek	Sheep Creek	Cable Creek	Fly Creek	Dale	Dale	Dale	Tower Mt.	Tower Mt.	Cable Creek	Johnson Rock
UTM N:	4990556	4985339	4993512	4986800	4991690	4996082	4994340	4986135	4985865	4986364	4990521	4986027	4994779	4995240
UTM E:	363151	370347	405152	385270	388800	372124	378229	352185	350991	353262	366551	367897	376238	389060
Age (Ma):			29.8	28.8							~ 28			22.4
SiO_2	47.37	55.36	49.82	64.26	68.37	76.85	77.72	77.31	75.17	75.44	79.65	76.93	77.11	68.03
Al_2O_3	15.44	16.67	17.18	16.61	15.46	14.14	14.78	12.95	14.59	13.73	11.58	12.85	12.65	16.71
TiO_2	4.60	1.03	1.67	0.85	0.51	0.17	0.13	0.08	0.22	0.19	0.09	0.12	0.07	0.69
FeO*	13.71	7.21	9.09	4.79	4.62	1.06	1.42	0.97	1.65	1.76	0.76	0.98	0.82	3.81
MnO	0.21	0.24	0.17	0.06	0.08	0.07	0.02	0.02	0.03	0.02	0.00	0.02	0.01	0.02
CaO	8.57	7.66	10.55	4.62	2.60	0.38	0.18	0.63	0.95	1.04	0.17	0.74	0.54	4.03
MgO	5.11	5.24	7.63	2.85	0.36	0.37	0.36	0.11	0.45	0.28	0.02	0.08	0.30	0.16
K_2O	1.59	1.27	0.84	2.05	3.14	4.72	4.12	5.78	4.52	4.42	4.32	5.78	4.61	1.89
Na_2O	3.26	3.99	2.76	3.73	4.73	2.26	1.25	2.13	2.40	3.09	3.38	2.49	3.86	4.41
P_2O_5	0.69	0.33	0.29	0.20	0.15	0.04	0.03	0.02	0.02	0.03	0.03	0.02	0.05	0.25
Ni	3	143	85	44	5	11	10	5	8	12	5	4	1	9
Cr	20	212	171	40	4	3	5	5	8	3	5	3	2	14
Sc	25	21	37	16	9	2	1	2	3	3	0	2	2	13
V	337	158	232	55	6	16	10	3	17	17	3	5	0	56
Ba	391	565	317	736	844	703	457	612	599	650	86	868	615	788
Rb	19	31	11	26	53	112	134	135	99	108	101	97	109	22
Sr	615	838	613	420	296	105	58	41	68	93	15	83	41	584
Zr	244	134	117	141	334	97	98	92	105	98	208	116	85	200
Y	31	16	21	17	35	21	18	19	20	20	34	15	21	18
Nb	40.3	15.3	18.7	16.0	41.0	16.8	17.4	13.2	13.4	17.2	30.1	12.0	19	16.5
Ga	26	18	19	18	26	19	29	16	18	15	25	15	16	23
Cu	18	28	85	25	1	6	6	6	10	9	5	5	5	11
Zn	121	67	80	56	115	19	31	33	40	33	70	30	18	82
Pb	4	7	16	6	9	5	10	14	13	12	14	12	14	7
La	24	10	†N.D.	21	45	24	30	35	29	27	39	27	50	20
Ce	58	43	36	55	86	70	53	57	56	43	66	45	41	48
Th	3	2	4	2	5	9	9	11	9	8	11	9	9	4
Nd	†N.D.	†N.D.	†N.D.	†N.D.	†N.D.	†N.D.	†N.D.	21	20	†N.D.	33	15	†N.D.	†N.D.

Note: Major element determinations have been normalized to a 100% total on a volatile-free basis and recalculated with total iron expressed as FeO*. Oxides as weight percent; trace elements as parts per million.

†N.D. = no data or element not analyzed.

around the caldera ceased around 22.4 Ma when dacite and andesite lavas erupted from vents located northeast of the caldera margin. Although the outflow sheet and northern and western margin to the caldera were later buried by basalt lavas of the Columbia River Basalt Group, the Tower Mountain caldera is well-defined by a geophysical signature that includes a large closed gravity low coincident with the caldera and by paired magnetic lows coincident with ring fracture rhyolite domes (Ferns et al., 2001).

Rocks of the Tower Mountain volcanic field are part of the "eastern" facies of the John Day Formation (Figs. 1 and 3); the Tuff of Dale is stratigraphically equivalent to the Turtle Cove Member. No distal tuffs, correlative to the Tuff of Dale and the Tower Mountain caldera, have yet been identified within the John Day Fossil Beds National Monument. The 27.89 ± 0.57 Ma Deep Creek Tuff ($^{40}Ar/^{39}Ar$, plagioclase) and the overlying 27.18 ± 0.13 Biotite Tuff (Albright et al., 2008) exposed north of the Sheep Rock Unit are similar in age to the Tuff of Dale, but geochemical analyses from these tuffs suggest they are chemically distinct units erupted from other unknown sources. The 28.9 Ma feldspar and hornblende-phyric Blue Basin Tuff (Bestland, 1995; Albright et al., 2008), a 1–2-m-thick airfall unit exposed in the Sheep Rock Unit, is also temporally correlative with the Tower Mountain caldera, but no samples of this tuff have yet been analyzed (Fig. 3).

Stop 3-1. The Tuff of Dale: Outflow Facies of the Tower Mountain Caldera [GPS coordinates –118.8915, 45.0119]

Stop 3-1 is at a scenic pullout along U.S. Forest Service (USFS) Road 55, where a road cut exposes the non-welded upper part of the outflow facies of the Tuff of Dale (Fig. 17). Below the road grade, more strongly welded ash-flow tuff weathers to precipitous white cliffs and blocky columns that tower more than 30 m above the North Fork of the John Day River. The tuff can be traced south beneath the middle Miocene Picture Gorge Basalt into the lower part of Desolation Creek, where the exposures have not yet been mapped in detail (Fig. 16). The Tuff of Dale is marked by conspicuous glassy porphyritic dacite and aphyric rhyolite lithics and flattened, perlitic fiamme. Phenocrysts include broken quartz, plagioclase and potassium feldspar, and sparse biotite. Geochemical analyses show the Tuff of Dale is characterized by typically low amounts of Nb, Y, and Zr (Table 4). Although the Tuff of Dale is presently undated, timing of the eruption is constrained by $^{40}Ar/^{39}Ar$ ages of 29.80 ± 0.39 Ma (whole rock) on a Ti-rich basalt lava that forms the base of the Tower Mountain volcanic field and 22.4 ± 0.16 Ma (whole rock) on a biotite dacite dome at the top of the section (Ferns et al.,

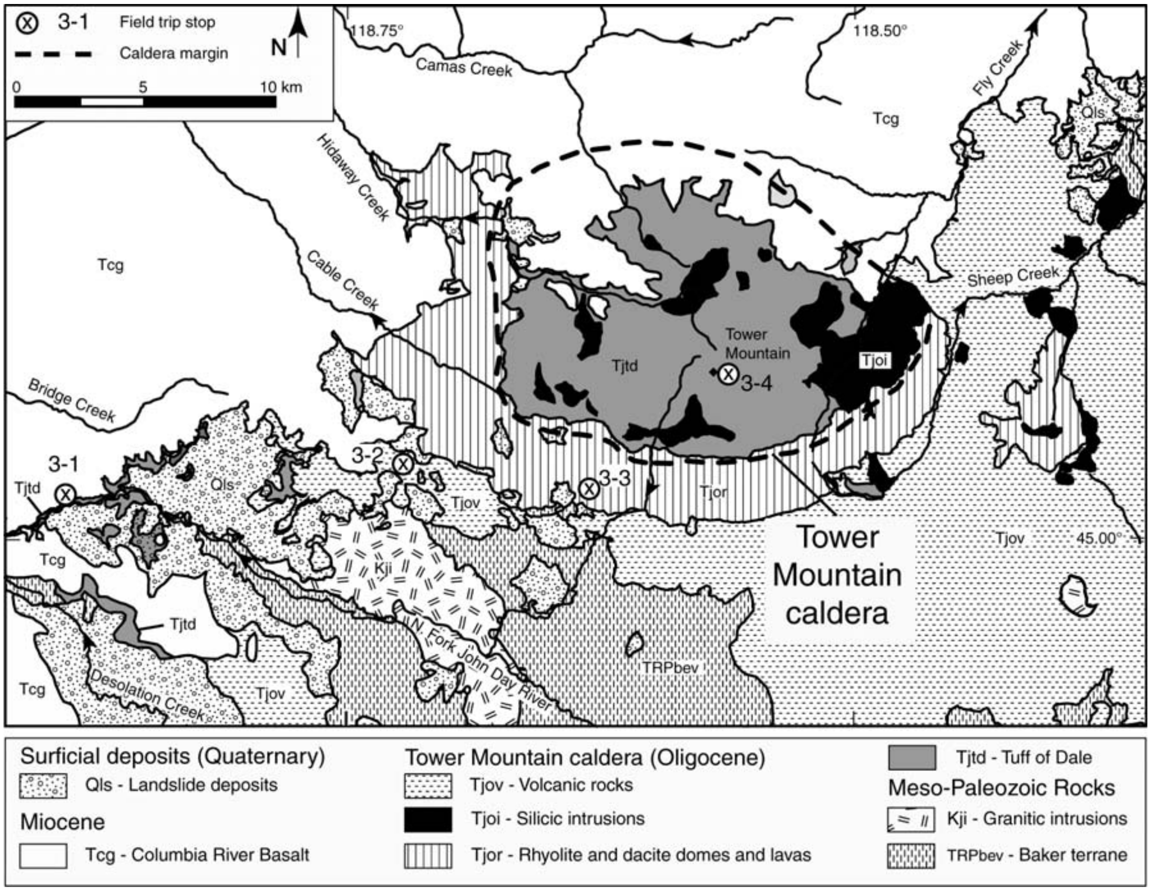

Figure 16. Simplified geologic map of the Tower Mountain caldera labeled with associated field stops.

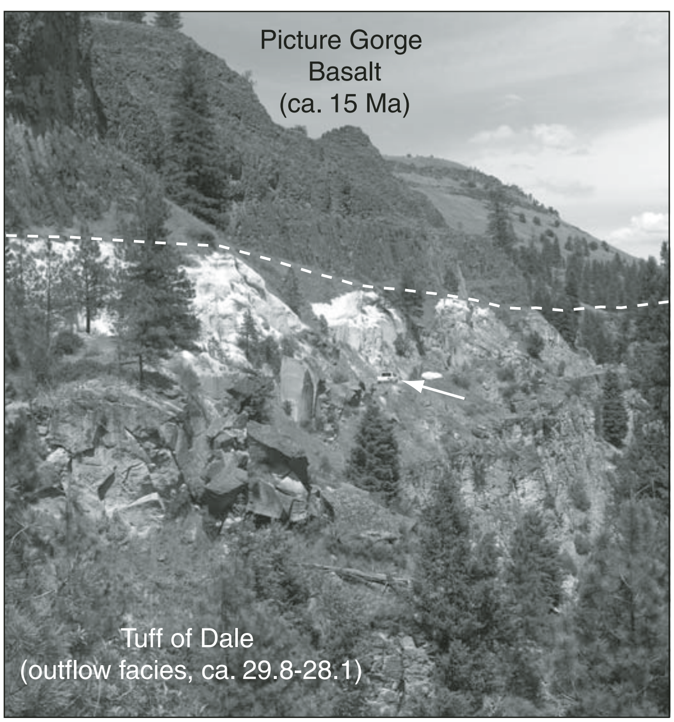

2001). An older K/Ar age of 28.1 ± 1.5 Ma on anorthoclase crystals from one of the post-collapse ring-fracture domes (Fiebelkorn et al., 1982) suggests that the Tower Mountain caldera formed at about the same time as the Crooked River caldera.

Stop 3-2. Tower Mountain Caldera Overlook [GPS coordinates –118.7237, 45.0273]

Stop 3-2 is a panoramic view looking across the encircling ring-fracture rhyolite dome complex into the resurgent core of the Tower Mountain caldera (Figs. 16 and 18). The timbered high point on the northeast is Tower Mountain, which is underlain by > 500 m of lithic-rich tuff preserved in the resurgent core of the caldera. The resurgent core is nearly 15 km in diameter and is cut by numerous dacite and rhyolite intrusions (Fig. 16). The low hills on the west and in the foreground on the south are part of a rhyolite

Figure 17. Outflow facies of the Tuff of Dale exposed along the North Fork of the John Day River at Stop 3-1. Dashed white line marks the contact between the tuff and overlying middle Miocene Picture Gorge Basalt. Arrow points to automobile for scale.

dome field that was extruded along the south and western margins to the caldera following the climactic eruption. Domes on the west flank are porphyritic and generally contain higher levels of Nb and Y than do the ash-flow tuff and aphyric rhyolite domes on the east (Table 4). The western and northern flanks of the domes are unconformably overlain by lavas of the Columbia River Basalt Group, which forms the more sparsely vegetated table lands.

The porphyritic dacite exposed at the overlook is typical of the early-stage silicic lavas and breccias that were erupted from Tower Mountain prior to the culminating ash-flow tuff eruption. Early stage silicic lavas are typically very porphyritic, containing up to 15% phenocrysts. Plagioclase up to 7 mm, hypersthene, and augite phenocrysts are the main phenocryst phases; however some flows contain quartz and olive green hornblende. Crystalline xenoliths of two pyroxene diorite occur in many of the dacite lavas. Proximal flow margins are marked by vitrophyre and intervening lobes of generally monolithologic matrix-supported breccia. More distal breccias contain a variety of clasts and, in places, petrified wood.

Following collapse of the Tower Mountain caldera, rhyolite flows, domes, plugs and dikes, geochemically similar to the Tuff of Dale, were emplaced along the southern and eastern structural margins and interior of the caldera (Fig. 16). The rhyolites either intrude or overlie the intracaldera facies. Elongation of some rhyolite dikes and domes parallel to the caldera margin suggests that these complexes were likely erupted from ring-fracture fissures. Other rhyolite intrusions and dikes are elongated in a northwest-southeast direction parallel to the dominant structural fabric observed in local faults and pre-caldera intermediate dikes. Many rhyolite dikes within the caldera are bordered by silicified breccia zones, some of which contain anomalous amounts of Hg. Precious opal is found in rhyolite at several places along the western margin, most notably near Hidaway Springs. Agate- and opal-filled geodes have also been found in the marginal rhyolite domes.

Stop 3-3. Ring-Fracture Rhyolite Domes [GPS coordinates –118.6319, 45.0173]

Stop 3-3 is near the contact between a largely aphyric rhyolite dome field that defines the south and eastern caldera margin and a largely porphyritic rhyolite dome field that defines the south and western caldera margin (Fig. 16). The aphyric domes are commonly marked by perlite and perlite breccia (Fig. 19A). Perlitic zones are characterized by myrmekitic cores of black obsidian that weather to rounded nodules similar to "Apache tears" (Fig 19B). Unlike the classical translucent Apache tears of Arizona and New Mexico, the tears at this locality are nearly opaque.

Aphyric and sanidine-phyric rhyolite domes along the south margin of the caldera are remarkably chemically similar to the Tuff of Dale. These rhyolites characteristically contain low amounts of Nb (10.8–12.0 ppm), Y (15–16 ppm), and Zr (97–116 ppm) (Table 4) and may represent viscous magmas that were emplaced along the southern caldera margin during the final stages of the culminating, caldera-forming eruption. Porphyritic rhyolite domes along the northwest margin to the caldera contain relatively higher amounts of Nb (26.2–30.1 ppm), Y (26–34 ppm), and Zr (133–208 ppm) (Table 3). The rhyolite dome complex that lies several miles east of the caldera margin contains the highest amounts of Nb (50 ppm), Y (20 ppm), and Zr (336 ppm) in the Tower Mountain volcanic field (Ferns, 1999).

Stop 3-4. The Tuff of Dale: Intracaldera Facies [GPS coordinates –118.5640, 45.0543]

The summit of Tower Mountain lies at the center of the resurgent core of the Tower Mountain caldera (Fig. 16). Here, zeolitized lithic tuff, which weathers to green chips, is cut by dacite, basalt, and rhyolite intrusions (Fig. 20). Although the core

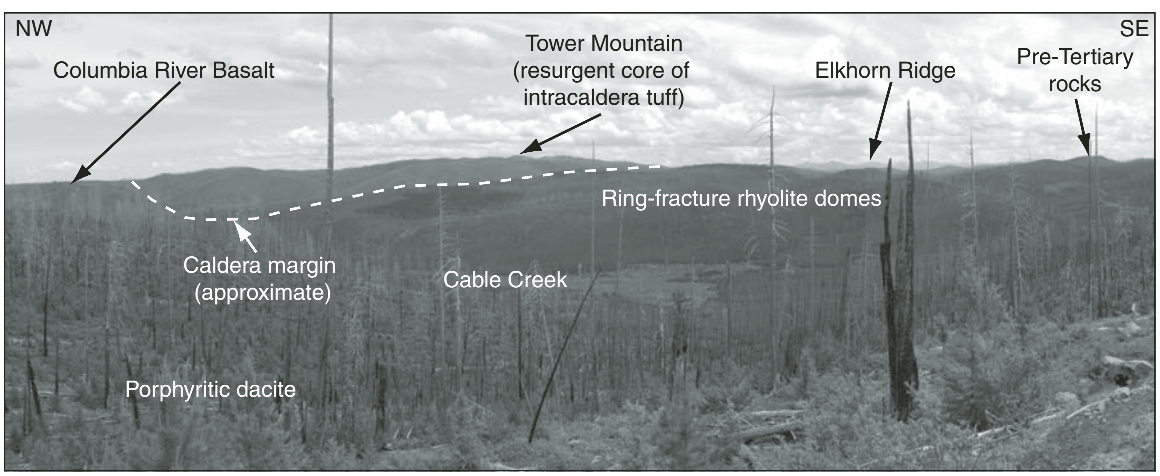

Figure 18. Panoramic view across the Tower Mountain caldera from Stop 3-2. The resurgent core to the caldera forms the high-skyline to the north-northeast. Dashed white line shows the approximate trace of the caldera margin. Ring-fracture dacite and rhyolite domes form the low-lying hills in the foreground. Lavas of the middle Miocene Columbia River Basalt Group unconformably overly the core of the caldera on the northwest. Pre-Tertiary rocks are exposed outside of the caldera margin on the southeast and along Elkhorn Ridge on the east, in the far distance.

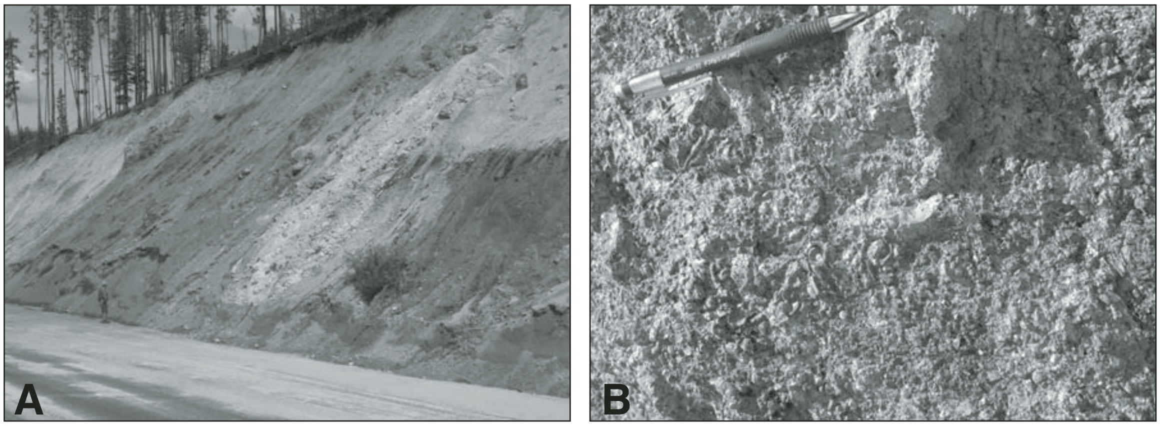

Figure 19. (A) Aphyric rhyolite dome marked by perlite and perlite breccia. Person for scale in lower left part of the photograph is 1.9 m tall (B) Perlitic zones are characterized by myrmekitic cores of black obsidian that weather to rounded nodules similar to "Apache tears." Pencil for scale in upper left part of the photograph is 14 cm long.

is densely forested and exposures are limited, torrential rains following the 1995 Tower Mountain fire formed hillside gullies west of here, in which more than 130 m of massive lithic tuff were temporarily exposed. The lithic tuff contains flattened pumices up to 15 cm in length and dacite porphyry clasts up to 12 cm in diameter. Along the western margin of the caldera, the tuff has compacted to such a degree that it displays secondary flow features typical of rheomorphic tuffs. Chemical and physical compositions of the intracaldera and outflow facies of the Tuff of Dale are identical (Table 4). Both contain quartz, plagioclase, potassium feldspar, and altered biotite phenocrysts, porphyritic dacite lithic fragments and nearly identical major and trace element compositions.

The summit of Tower Mountain provides a panoramic view of the Blue Mountains (Fig. 20). The heavily glaciated mountains on the east and south mark the western terminus of Elkhorn Ridge. These mountains are cored by the late Jurassic to early Cretaceous Bald Mountain Batholith. In the distance on the south lies Strawberry Mountain, a middle Miocene calc-alkaline vent that began forming shortly after the massive eruptions of the Columbia River Basalt Group. In the foreground on the south lies the Greenhorn Mountains, a fault block that is largely cored by pre-Tertiary mélange and younger Mesozoic intrusions. The lower elevation country immediately to the east of the Greenhorn Mountains is composed of deeply eroded Paleogene volcanic and volcaniclastic rocks. These rocks are part of the middle Eocene to early Oligocene calc-alkaline Cougar Rock volcanic field that lies ~40 km south of Tower Mountain (Fig. 1). Radiometric $^{40}Ar/^{39}Ar$ ages by Urbanczyk (1994) place the onset of volcanism in the Cougar Rock volcanic field at 43.5 ± 0.4 Ma with cessation of activity around 33.6 ± 0.3 Ma. The initial volcanic pulse in the Cougar Rock volcanic field was therefore contemporaneous with similar calc-alkaline eruptions in the middle Eocene Ochoco volcanic field further west.

ROAD LOG

The field trip leaves from the Oregon Convention center in Portland. The detailed road log for the field trip begins at the north end of Madras at the intersection of U.S. 26 and U.S. 97 (Fig. 2). While a majority of this field trip travels over major paved highway and secondary roads, sections of the route do traverse over unpaved USFS forest roads at higher elevations that may be impassable in the late fall, winter, and early spring. Please check with the USFS for current road conditions on the Ochoco and Umatilla National Forest before embarking on the trip. Independent readers of this guide are encouraged to carry a detailed Oregon road atlas to aid in navigation along the field

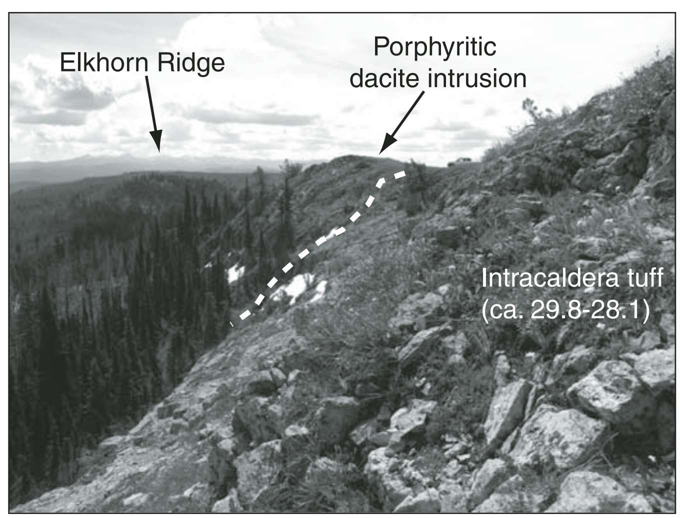

Figure 20. Intracaldera tuff intruded by a post-subsidence porphyritic dacite intrusion along the summit of Tower Mountain at Stop 3-4. Dashed white line shows the approximate contact between the tuff and the intrusion. Elkhorn Ridge is visible in the distance to the southeast.

trip route. GPS coordinates, recorded in longitude and latitude (NAD 27, deg.dddd), are given to aid in navigation to each field stop. Azimuth directions are given at some stops to point out the geographic orientation of features described in the text.

Directions from the Oregon Convention Center to Madras

Cumulative mileage	*(km)*	*Description*
0.0	(0.0)	Leave the Oregon Convention center and go south on NE Martin Luther King Jr. Boulevard/OR 99E toward NE Irving Street.
0.2	(0.3)	Turn left onto NE Everett Street.
0.3	(0.5)	Merge onto I-84 E towards the Portland Airport/The Dalles. Drive east to exit 16.
13.2	(21.2)	Take exit 16/238th Drive toward Wood Village.
13.5	(21.7)	Turn right onto NE 238th Drive.
14.5	(23.3)	NE 238th Drive becomes NE 242nd Drive.
15.1	(24.3)	NE 242nd Drive becomes NE 242nd Avenue.
16.3	(26.2)	Turn slightly left onto NE Burnside Road.
16.6	(26.7)	NE Burnside Road becomes SE Burnside Street.
17.0	(27.4)	SE Burnside Street becomes U.S. 26 E/ Mt. Hood Highway. Drive 101.4 mi on U.S. 26 E to Madras.
118.4	(190.5)	Madras.

DAY 1. THE CROOKED RIVER CALDERA

Cumulative mileage	*(km)*	*Description*
0.0	(0.0)	Intersection of U.S. 26 and U.S. 97 at the north end of Madras [GPS coordinates –121.1285, 44.6403]. Set trip odometer to zero and proceed south on U.S. 97.
2.1	(3.4)	U.S. 97 leaves Madras.
2.4	(3.9)	Junction with U.S. 26; continue south on U.S. 97
3.5	(5.6)	The near ridgeline on the east is composed of a west-dipping section of Oligocene tuffs, sedimentary rocks, and lavas that are part of the “western” facies of the John Day Formation (Robinson, 1975; Robinson et al., 1990). Part of this section includes outflow tuff of the Crooked River caldera. The high ridge in the distance on the east is composed of rocks of the Eocene Clarno Formation.
10.1	(16.3)	Intersection of U.S. 26 and Jericho Lane. The butte visible on the southwest is Juniper Butte, an outlier Oligocene rhyolite dome related to the Crooked River caldera. The ridge visible on the southeast is composed of strongly welded to rheomorphic ash-flow tuff that is part of the outflow facies of the Tuff of Smith Rock (Fig. 4).
11.8	(19.0)	Haystack Butte, the flat-topped mesa visible on the southeast, is capped by the Tuff of Barnes Butte. This ash-flow tuff is underlain by Oligocene sedimentary rocks and outflow tuff facies of the Tuff of Smith Rock (Fig. 4).
17.8	(28.6)	Crossing the U.S. 97 bridge over the Crooked River Gorge.
18.0	(29.0)	Turn right into Peter Skene Ogden State Park.
18.1	(29.1)	Parking area for Stop 1-1.

Stop 1-1. Northwest Margin of the Crooked River Caldera at Peter Skene Ogden State Park [–121.1928, 44.3929]

Park and walk 0.1 mi northeast along the developed paths to the overlook on the old U.S. 97 highway bridge. The ridgeline visible on the east is composed of John Day Formation strata that compose part of the northwest margin of the Crooked River caldera (Fig. 6). Restroom facilities are available.

18.2	(29.3)	Exit the park and turn right onto U.S. 97.
18.7	(30.1)	Coyote Butte, visible on the east is composed of intracaldera facies of the Tuff of Smith Rock. The margin of the Crooked River caldera here is inferred to arc between the Coyote Butte and U.S. 97, but is now buried by Neogene basalt lavas (Fig. 4).
21.1	(34.0)	Terrebonne; turn left on B Ave/Smith Rock Way.
21.8	(35.1)	Turn left on 1st Street.
22.3	(35.9)	1st Street turns sharply to the east and becomes NE Wilcox Avenue.
23.8	(38.3)	Turn left onto Crooked River Drive and proceed to the main overlook area.
24.4	(39.3)	Parking area for Stop 1-2.

Stop 1-2. The Tuff of Smith Rock: Intracaldera Facies at Smith Rock State Park [–121.1349, 44.3669]

From the main overlook, a short 1 mi roundtrip hike down the well-maintained trail and across the footbridge over the Crooked River reaches cliffs composed of the Tuff of Smith Rock (Fig 7). Restroom facilities are available.

25.1	(40.4)	Exit the park and turn left onto NE Wilcox Avenue.
28.1	(45.2)	Turn left onto Smith Rock Way.
28.6	(46.0)	Turn left onto NW Lone Pine Road (caution, be aware of gravel trucks).
28.9	(46.5)	Crossing the Crooked River.
30.1	(48.4)	Gray Butte, an Oligocene rhyolite dome complex, forms the prominent peak on the northwest. The Tuff of Smith Rock and post-subsidence rhyolite intrusions are visible in the foreground (Fig. 4).

36.0	(57.9)	Turn right onto U.S. 26. Grizzly Mountain, an Oligocene rhyolite dome complex, forms the high skyline on the east. Proceed 3.3 mi south to Grizzly Mountain Road (Fig. 4).
39.3	(63.2)	Turn left onto Grizzly Mountain Road and proceed to the undeveloped parking area on the lower summit of Grizzly Mountain.
42.1	(67.8)	Parking area for Stop 1-3.

Stop 1-3. Rhyolite of Grizzly Mountain: Post-Collapse Ring-Fracture Rhyolite Domes [–120.9578, 44.4317]

Park in the undeveloped circular parking area on the left side of the road. A short 0.2 mi hike south up a jeep-trail reaches a panoramic viewpoint and outcrops of the rhyolite (Fig. 8)

44.1	(71.0)	Retrace route back to U.S. 26. Turn left onto U.S. 26 and continue south into Prineville.
53.6	(86.3)	Junction with OR 126. Yield to oncoming traffic and proceed east on U.S. 26 (3rd Street) through Prineville.
55.1	(88.7)	Combs Flat Crossing at the east end of Prineville. Turn right onto Combs Flat Road. Barnes Butte is visible on the northeast. The southern part of the butte is capped by the planiform outcropping Tuff of Barnes Butte, an ash-flow tuff erupted from within the southeastern confines of the Crooked River caldera between 29.56 and 27.97 Ma (Fig. 4). It is not clear whether eruption of the Tuff of Barnes Butte resulted in the formation of a second collapse structure or whether it erupted from another type of vent structure (e.g., ignimbrite fissure; Aguirre-Díaz and Labarthe-Hernández, 2003). No topographic expression of a subsidiary caldera ring-structure is clearly defined. The northern part of Barnes Butte is a rhyolite dome complex, isotopically dated at 27.97 ± 0.32 Ma ($^{40}Ar/^{39}Ar$ whole rock; McClaughry and Ferns, 2006a), that intrudes the overlying Tuff of Barnes Butte. The rhyolite intrusion is geochemically indistinguishable from the Tuff of Barnes Butte identifying this area as the eruptive source (Table 1).
56.5	(90.9)	Turn right onto Juniper Canyon Road.
69.1	(111.2)	Turn right onto County Boat Ramp Road.
70.5	(113.5)	Parking area for Stop 1-4.

Stop 1-4. Pre-Caldera Volcanic Stratigraphy at Prineville Reservoir County Boat Ramp [–120.7487, 44.1330]

A short walk east (0.5 mi) from the boat ramp, along the south side of the reservoir traverses outcrops of northwest dipping interbedded tuffs and tholeiitic basalt lavas exposed just outside of the southern margin of the Crooked River caldera (Fig. 9). Restrooms are available at the boat ramp.

85.9	(138.2)	Retrace route 15.4 mi back to Combs Flat Crossing in Prineville. Combs Flat Crossing in Prineville. End of Day 1.

DAY 2. THE WILDCAT MOUNTAIN CALDERA AND JOHN DAY FOSSIL BEDS NATIONAL MONUMENT

Cumulative mileage	*(km)*	*Description*
85.9	(138.2)	The Day 2 road log begins at the intersection of U.S. 26 and Combs Flat Road in Prineville.
89.9	(144.6)	The 27.54 ± 0.36 Ma Rhyolite of Ochoco Reservoir, exposed north of the highway is a south-dipping, sanidine-phyric rhyolite lava that erupted along the southeast margin of the Crooked River caldera following the main subsidence phase (Fig. 4; McClaughry and Ferns, 2006b). The rhyolite overlies sedimentary rocks interpreted as moat-fill deposits
92.3	(148.5)	Ochoco Lake County Park on the right.
92.9	(149.5)	Crossing the southeast ring-fracture zone of the Oligocene Crooked River caldera.
94.3	(151.8)	Turn left onto Mill Creek Road (USFS Road 33); drive north to Stop 2-1.
96.5	(155.3)	The Rhyolite of Mill Creek is exposed on the west side of the road (Fig. 10). This rhyolite also caps Mahogany Butte, visible 2 mi north-northeast of this point. The rhyolite forms a northeast trending outcrop belt across the southeast part of the Wildcat Mountain caldera where it intrudes intracaldera facies of the Tuff of Steins Pillar.
97.9	(157.5)	An ~ 8 m thick, N50°W trending, vertical dike of hornblende- and plagioclase-phyric dacite is exposed in the rock quarry on the left. The dike, which has an Ar^{40}/Ar^{39} age of 42.79 ± 0.44 Ma (hornblende, McClaughry and Ferns, 2006b), forms part of the basement to the Wildcat Mountain caldera.
102.5	(165.0)	Parking area for Stop 2-1 is on the right side of the road (Figs. 10 and 11).

Stop 2-1. Steins Pillar Viewpoint [–120.6176, 44.4173]

103.9	(167.2)	Turn left out of parking area and retrace USFS Road 33 south, 1.4 mi to USFS Road 3300-500. Turn left onto USFS Road 3300-500. Cross Mill Creek and continue 3.2 mi east to Stop 2-2.
106.0	(170.6)	Parking area for Stop 2-2. Park behind the berm that blocks the road.

Stop 2-2. The Tuff of Steins Pillar and Post-Subsidence Rhyolite Dikes [–120.6216, 44.3932]

A short 0.3 mi walk up the closed section of the road provides good exposure of intracaldera tuff and post-subsidence rhyolite dikes that intrude the tuff (Figs. 10 and 12).

108.1 (174.0) Retrace the route along USFS Road 3300-500 back to USFS Road 33. Turn right onto USFS Road 33 and proceed north.
109.5 (176.2) Steins Pillar viewpoint.
112.0 (180.2) Access road to Wildcat Campground on the right. Continue left on USFS Road 33.
116.3 (187.2) Harvey Gap. Turn right on USFS Road 3320. Porphyritic andesite exposed in the quarry north of the intersection forms part of the basement to the Wildcat Mountain caldera. A sample from this quarry has an $^{40}Ar/^{39}Ar$ age of 43.86 ± 0.89 Ma (plagioclase, Ferns and McClaughry, 2007), which marks the onset of magmatism in this part of the Ochoco volcanic field.
120.6 (194.1) Parking area for Stop 2-3. Pull off and park in the pullout on the right side of the road, just past the rhyolite roadcut (Figs. 10 and 13).

Stop 2-3. The Rhyolite of Hash Rock and Twin Pillars Viewpoint [–120.5723, 44.4955]

121.2 (195.1) Continue north on USFS Road 3320; turn right on USFS Road 27 and travel 2.2 mi east to Trail Meadows. (Please note the route across USFS Road 27 may at times be impassable due to fallen trees blown down during frequent high-energy wind storms across this part of the Ochoco Mountains.)
123.4 (198.6) Trail Meadows, keep right on USFS Road 27.
124.2 (199.9) Bingham Prairie. Twin Pillars trailhead is on the left. Continue 3.0 mi east on USFS Road 27 from the Twin Pillars trailhead to the intersection with USFS Road 200/Whistler Road.
127.1 (204.5) Turn left onto USFS Road 200/Whistler Road.
131.6 (211.8) Turn right on USFS Road 2730. Proceed to the intersection with U.S. 26.
142.6 (229.5) Turn left onto U.S.26. Travel east toward Mitchell.
143.2 (230.4) Ochoco Divide. Descending into the John Day Basin.
147.8 (237.8) Two conical buttes visible on the south are dacite plugs that intrude Cretaceous marine rocks. Black Butte, in the foreground, is flanked by a series of andesite and phlogopite-bearing lamprophyre dikes that have $^{40}Ar/^{39}Ar$ ages of 48.97 ± 0.14 Ma and 48.65 ± 0.14 Ma (phlogopite, Appel, 2001). The butte in the distance is White Butte, a dacite intrusion which has a K/Ar age of 41.6 ± 0.9 Ma (whole rock, Enlows and Parker, 1972; Fiebelkorn et al., 1982). Both Black and White Butte are considered to be part of the Eocene Clarno Formation.
148.2 (238.5) Folded and faulted Cretaceous Gables Creek and Hudspeth Formations.
152.0 (244.6) Highway 26 cuts through a series of alkali basalt intrusions that have a whole rock $^{40}Ar/^{39}Ar$ age of 45.26 ± 0.31 Ma (Appel, 2001). The dikes intrude a section of poorly exposed volcaniclastic rocks that here define the base of the Clarno Formation.
154.9 (249.2) The rim-rock south of the highway is an ash-flow tuff in the Clarno Formation. Age, geochemical affinities, and stratigraphic position of this tuff are presently undetermined.
155.5 (250.3) Turn left onto Burnt Ranch Road and drive north to Painted Hills Unit of the John Day Fossil Beds National Monument.
157.0 (252.6) North-dipping section of porphyritic andesite lavas for which Appel (2001) reports a whole rock $^{40}Ar/^{39}Ar$ age of 42.9 ± 0.2 Ma.
160.9 (258.5) Turn left onto gravel access road into the Painted Hills Unit. Continue west.
161.3 (259.6) Keep to the right and proceed to the viewpoint area. Public restrooms and a picnic area are available at the park on the left.
162.1 (260.9) Parking area for Stop 2-4.

Stop 2-4. Painted Hills Unit, Carroll Rim Trail and Viewpoint [–120.2662, 44.6522]

The Carroll Rim trailhead is near the road junction and parking area for the Painted Hills overlook. A moderately strenuous 0.5 mi hike ascends Carroll Rim on the northeast and offers a spectacular viewpoint of the Painted Hills and outcrops of fallout and ash-flow tuffs that are part of the Turtle Cove Member (“eastern” facies) of the John Day Formation (Fig. 14). A short walk up the hill to the south reaches the Painted Hills overlook which views the red banded badland hills of the older Big Basin Member.

163.3 (262.8) Exit the Painted Hills Unit and turn right onto Burnt Ranch Road. Retrace the route back to U.S. 26.
168.7 (271.5) Turn left onto U.S. 26; proceed east toward John Day.
169.9 (273.4) Mafic dike intruding Cretaceous marine rocks. The red-weathering dike in the center of the valley on the north has a whole rock K/Ar age of 33.3 ± 1.2 Ma (Enlows and Parker, 1972; Taylor, 1981). These dikes are high-Ti tholeiitic basalts that chemically

resemble intrusions and lavas associated with the Crooked River caldera.

172.8 (278.1) Mitchell.

175.1 (281.7) The west-northwest–trending Keyes Creek dike cuts a section of Clarno Formation volcaniclastic breccia. The dike is a high-Ti tholeiitic basalt (Taylor, 1981) that has a whole rock $^{40}Ar/^{39}Ar$ age of 34.1 ± 0.6 Ma (Appel, 2001).

179.6 (289.0) Keyes Summit. The rolling hills in foreground on the north are eroded andesite and dacite lavas in the Clarno Formation.

204.9 (329.8) Turn left onto OR 19 towards Kimberly, and proceed north to the Sheep Rock Unit of the John Day Fossil Beds National Monument.

207.0 (331.1) Turn left into the parking area for the visitor center.

Stop 2-5. Sheep Rock Unit and Thomas Condon Paleontology Center [–119.6437, 44.5531]

The Thomas Condon Paleontology Center in the Sheep Rock Unit of the John Day Fossil Beds National Monument features exhibits that showcase some of the spectacular paleontological specimens that have been recovered from the John Day Formation. A short hike up the trail that begins near the south end of the parking area ascends to a nice overlook of Sheep Rock, which here towers above the John Day River (Fig. 15). Restroom facilities are available.

207.1 (333.3) Leave parking area and turn right on OR 19. Drive south to U.S. 26.

209.2 (336.7) Left turn on U.S. 26; drive east through Picture Gorge to John Day.

216.0 (347.6) Dayville.

239.0 (384.6) Mount Vernon.

247.3 (398.0) Intersection of U.S. 26 and U.S. 395 in John Day. End of Day 2.

DAY 3. THE TOWER MOUNTAIN CALDERA

Cumulative mileage	*(km)*	*Description*
247.3	(398.0)	The Day 3 road log begins at the intersection of U.S. 26 and U.S. 395 in John Day. Travel west on U.S. 26 to Mount Vernon.
255.6	(411.3)	Turn right onto U.S. 395. Proceed north to Dale.
275.4	(443.2)	Beech Creek.
285.6	(459.6)	Long Creek.
294.8	(474.4)	Ritter Butte Summit.
298.4	(480.2)	Crossing the Middle Fork of the John Day River.
310.7	(500.0)	Dale.
312.0	(502.1)	Turn right onto USFS Road 55 just after crossing the U.S. 395 bridge over the North Fork of the John Day River. Proceed east to Stop 3-1 (Fig. 16).
315.2	(507.3)	Parking area for Stop 3-1. Park in available pullouts on the right side of the road.

Stop 3-1. The Tuff of Dale: Outflow Facies [–118.8915, 45.0119]

The white tuff is well-exposed in roadcuts for several miles along USFS Road 55 (Figs. 16 and 17).

324.7 (522.6) Continue east on USFS Road 55 to the intersection with USFS Road 52. Turn right onto USFS Road 52 and continue east.

327.6 (527.2) Pearson Guard Station on the right.

328.1 (528.0) Parking area for Stop 3-2. Park in the pullout, monumented by a highway marker labeled "auto tour, stop 4," on the left side ~0.5 mi past Pearson Guard Station.

Stop 3-2. Tower Mountain Caldera Overlook [–118.7237, 45.0273]

Porphyritic dacite is exposed in outcrop on the south side of the road, opposite the parking area (Figs. 16 and 18).

331.2 (532.9) USFS Road 52 skirts the contact between a series of post-collapse porphyritic rhyolite domes that were emplaced along the ring-fracture. The margins of the domes here overlie a sequence of white fallout tuff, lithic tuff, and porphyritic rhyolite breccias that rest on pre-Tertiary basement rocks.

333.0 (535.8) The base to the porphyritic rhyolite domes are in places marked by prominent banded vitrophyres that display distinctive flow fold textures.

334.0 (537.5) The road makes a large bend back to the south at the head of Winom Meadows.

334.4 (538.2) Parking area for Stop 3-3. Continue past the large roadcut on the left and park in the pullout on the left side of the road (Figs. 16 and 19).

Stop 3-3. Ring-fracture Rhyolite Domes [–118.6319, 45.0173]

336.0 (540.7) Proceed 1.6 mi south on USFS Road 52; turn left onto USFS Road 5226 and travel north.

342.9 (551.7) USFS Road 5226 crosses a swale that marks the contact between a flow-banded aphyric rhyolite ring-fracture dome and the caldera-filling tuff (Fig. 16).

344.2 (553.9) Tower Mountain fire lookout is on the right. Keep right and then immediately turn left onto USFS Road 210. Continue 0.2 mi to the end of the road and the summit overlook of Tower Mountain.

344.4 (554.3) Parking area for Stop 3-4. Park in the open area at the end of the road, (Figs. 16 and 20).

Stop 3.4 Tower Mountain Summit Overlook [–118.5640, 45.0543]

The intracaldera tuff and post-subsidence dacite intrusions are well-exposed on the north and east sides of the summit (Fig. 20).

344.6 (554.6) Retrace route to the Tower Mountain fire lookout and USFS Road 5226. Keep right and proceed north on USFS Road 5226 to OR 244.

345.3 (555.6) Intracaldera tuff exposed along USFS Road 5226.

347.3 (558.8) USFS Road 5226 crosses a small porphyritic dacite dike that intrudes the intracaldera tuff.

348.4 (560.6) USFS Road 5226 crosses a small mass of aphyric rhyolite that intrudes the intracaldera tuff. The margins to some of the aphryic rhyolite intrusions are silicified and locally brecciated, and may contain elevated levels of the pathfinder elements mercury and arsenic.

359.9 (579.2) Turn left onto OR 244 and proceed west towards Ukiah and U.S. 395.

376.6 (606.1) Ukiah.

378.8 (609.6) Turn right onto U.S. 395. Proceed north to Pendleton.

404.5 (651.0) Intersection of U.S. 395 and OR 74; keep right continuing northeast on U.S. 395

425.3 (684.5) I-84 interchange in Pendleton. Proceed westbound on I-84, 206.5 mi to the convention center in Portland.

631.8 (1016.8) Oregon Convention Center. End of Day 3.

End of road log.

ACKNOWLEDGMENTS

This field trip guide is a product of regional geologic mapping that was partially funded by the U.S. Geological Survey National Cooperative Geologic Mapping program under assistance award nos. 98HQAG2037 during 1998 and 05HQAG0037 and 06HQAG0027 during 2005 and 2006. Funding for geologic mapping was also provided by the State of Oregon. Additional financial support for geochemical and geochronological analyses was provided by the Oregon Water Resources Department, U.S. Forest Service Ochoco, Wallowa-Whitman, and Umatilla National Forests, and the Boise Corporation. Geochemical analyses reported for tuffs within the John Day Fossil Beds National Monument were collected under permit number JODA-2009-SCI-0001. Discussions of the regional Paleogene stratigraphy with Ted Fremd and regional geochemical analyses provided by Paul Hammond are greatly appreciated. Graham Andrews, Greg Retallack, and Ian Madin contributed valuable critical reviews that improved the final manuscript.

REFERENCES CITED

Aguirre-Díaz, G.J., and Labarthe-Hernández, G.L., 2003, Fissure ignimbrites: Fissure-source for voluminous ignimbrites of the Sierra Madre Occidental and its relationship with Basin and Range faulting: Geology, v. 31, p. 773–776, doi: 10.1130/G19665.1.

Albright, L.B., III, Woodburne, M.O., Fremd, T.J., Swisher, C.C., III, MacFadden, B.J., and Scott, G.R., 2008, Revised chronostratigraphy and biostratigraphy of the John Day Formation (Turtle Cove and Kimberly Members), Oregon, with implications for updated calibration of the Arikareean North American Land Mammal Age: The Journal of Geology, v. 116, p. 211–237, doi: 10.1086/587650.

Appel, M., 2001, Alkaline and peraluminous intrusives in the Clarno formation around Mitchell, Oregon: Ramifications on magma genesis and subduction tectonics [M.S. thesis] Corvallis, Oregon State University, 222 p.

Ashwill, M.S., 1983, Seven fossil floras in the rain shadow of the Cascade Mountains, Oregon: Oregon Geology, v. 45, p. 107–111.

Best, M.G., Christiansen, E.H., and Blank, R.H., Jr., 1989, Oligocene caldera complex and calc-alkaline tuffs and lavas of the Indian Peak volcanic field, Nevada and Utah: Geological Society of America Bulletin, v. 101, p. 1076–1090, doi: 10.1130/0016-7606(1989)101<1076:OCCACA>2.3.CO;2.

Bestland, E.A., 1995, Stratigraphy of the Turtle Cove Member of the John Day Formation at Sheep Rock: U.S. National Park Service Open-File Report, 14 p.

Bestland, E.A., and Retallack, G.J., 1994a, Geology and paleoenvironments of the Clarno Unit, John Day Fossil Beds National Monument, Oregon: U.S. National Park Service Open-File Report, 160 p.

Bestland, E.A., and Retallack, G.J., 1994b, Geology and paleoenvironments of the Painted Hills Unit, John Day Fossil Beds National Monument, Oregon: U.S. National Park Service Open-File Report, 211 p.

Bestland, E.A., Hammond, P.E., Blackwell, D.L.S., Kays, M.A., Retallack, G.J., and Stimac, J., 1999, Geologic framework of the Clarno Unit, John Day Fossil Beds National Monument: Central Oregon: Oregon Geology, v. 61, p. 3–19

Brooks, H.C., 1963, Quicksilver in Oregon: Oregon Department of Geology and Mineral Industries Bulletin 55, 223 p.

Brown, D.E., Black, G.L., McLean, G.D., and Petros, J.R., 1980, Preliminary geology and geothermal resource potential of the Powell Buttes area, Oregon: Oregon Department of Geology and Mineral Industries Open-File Report O-80-8, 117 p.

Christiansen, R.L., 2001, The Quaternary and Pliocene Yellowstone Plateau volcanic field of Wyoming, Idaho, and Montana: U.S. Geological Survey Professional Paper 729-G, 145 p.

Christiansen, R.L., and Yeats, R.S., 1992, Post-Laramide geology of the U.S. Cordilleran region, *in* Burchfield, B.C., Lipman, P.W., and Zoback, M.L., eds., The Cordilleran Orogen: Conterminous U.S.: Geological Society of America, The Geology of North America, v. G-3, p. 261–406.

Coleman, R.G., 1949, The John Day Formation in the Picture Gorge Quadrangle, Oregon [M.S. thesis]: Corvallis, Oregon State University, 211 p.

Enlows, H.E., and Parker, D.J., 1972, Geochronology of the Clarno igneous activity in the Mitchell quadrangle, Wheeler County, Oregon: Ore Bin, v. 34, p. 104–110.

Evans, S.H., and Brown, F.H., 1981, Summary of potassium/argon dating —1981: U.S. Department of Energy, Division of Geothermal Energy DE-AC07-80-ID-12079-45, 29 p.

Evernden, J.F., and James, G.T., 1964, Potassium-argon dates and the Tertiary floras of North America: American Journal of Science, v. 262, p. 145–198.

Evernden, J.F., Savage, D.E., Curtis, G.H., and James, G.T., 1964, Potassium-argon dates and the Tertiary faunas of North America: American Journal of Science, v. 262, p. 145–198.

Ferns, M.L., 1999, Geologic map of the Fly Valley 7.5′quadrangle, Union County, Oregon: Oregon Department of Geology and Mineral Industries Geological Map Series GMS-113, scale 1:24,000.

Ferns, M.L., and McClaughry, J.D., 2007, Preliminary geologic map of the Hensley Butte and Salt Butte 7.5′ quadrangles, Crook County, Oregon: Oregon Department of Geology and Mineral Industries Open-File Report O-07-11, scale 1:24,000.

Ferns, M.L., Madin, I.P., and Taubeneck, W.H., 2001, Reconnaissance Geologic Map of the La Grande 30′ × 60′ quadrangle, Baker, Grant, Umatilla, and Union Counties, Oregon: Oregon Department of Geology and Mineral Industries Reconnaissance Map Series, RMS-1, 52 p., scale 1:100,000.

Fiebelkorn, R.B., Walker, G.W., MacLeod, N.S., McKee, E.H., and Smith, J.G., 1982, Index to K/Ar age determinations for the state of Oregon: Isochron-West, no. 37, p. 3–60.

Fisher, R.V., 1966, Geology of a Miocene ignimbrite layer, John Day Formation, Eastern Oregon: University of California Publications in Geological Sciences, v. 67, 58 p.

Fisher, R.V., and Rensberger, J.M., 1972, Physical stratigraphy of the John Day Formation, central Oregon: University of California Publications in Geological Sciences, v. 101, p. 1–45.

Gray, J.J., and Baxter, G., 1986, A reinterpretation of the Gray Butte limestone and arenite exposure as a hydrothermally-derived calcite vein and pebble dike: Oregon Geology, v. 48, p. 45–46.

Hladky, F.R., 1996, Geology and mineral resource map of the Grizzly Peak quadrangle, Jackson County, Oregon: Oregon Department of Geology and Mineral Industries Geological Map Series, GMS-106, scale 1:24,000.

Hladky, F.R., and Wiley, T.J., 1993, Ancient caldera complex revealed: Oregon Geology, v. 55, p. 70.

Honn, D.K., and Smith, E.I., 2007, Nested calderas in the Northern Kawich Range, Central Nevada: termination of the ignimbrite flare-up in the Great Basin: American Geophysical Union, Fall Meeting 2007, abstract #V41A-10.

Kauffman, J.D., Bush, J.H., and Lewis, R.S., 2003, Newly identified Oligocene alkali volcanics along the eastern margin of the Columbia Plateau, Latah and surrounding counties, Idaho: Geological Society of America Abstracts with Programs, v. 35, no. 6, p. A549.

Leonard, B.F., and Marvin, R.F., 1982, Temporal evolution of the Thunder Mountain caldera and related features, central Idaho, *in* Bonnichsen, W., and Breckenridge, R.M., eds., Cenozoic Geology of Idaho: Idaho Bureau of Mines and Geology, Bulletin 26, p. 23–41.

Lipman, P.W., 1984, Roots of ash-flow calderas in western North America: windows into the tops of granitic batholiths: Journal of Geophysical Research, v. 89, p. 8801–8841.

Ludington, S., Cox, D.P., Leonard, K.W., and Moring, B.C., 1996, Cenozoic volcanic geology of Nevada, *in* Singer, D.A., ed., An analysis of Nevada's metal-bearing mineral resources: Nevada Bureau of Mines and Geology Open-File Report 96-2, scale 1:1,000,000.

Manchester, S.R., 1981, Fossil plants of the Eocene Clarno Nut Beds: Oregon Geology, v. 43, p. 75–81.

Marsh, O.C., 1875, Ancient lake basins of the Rocky Mountains region: American Journal of Science, v. 9, p. 49–52.

Mathis, A.C., 1993, Geology and petrology of a 26-Ma trachybasalt to peralkaline rhyolite suite exposed at Hart Mountain, southern Oregon [M.S. thesis]: Corvallis, Oregon State University, 141 p.

McClaughry, J.D., and Ferns, M.L., 2006a, Preliminary geologic map of the Prineville 7.5′ quadrangle, Crook County, Oregon: Oregon Department of Geology and Mineral Industries Open-File Report O-06-22, scale 1:24,000.

McClaughry, J.D., and Ferns, M.L., 2006b, Preliminary geologic map of the Ochoco Reservoir 7.5′ quadrangle, Crook County, Oregon: Oregon Department of Geology and Mineral Industries Open-File Report O-06-23, scale 1:24,000.

McClaughry, J.D., and Ferns, M.L., 2007, The Crooked River Caldera: identification of an early Oligocene eruptive center in the John Day Formation of central Oregon: Geological Society of America Abstracts with Programs, v. 39, no. 4, p. A10.

McIntyre, D.H., Ekren, E.B., and Hardyman, R.F., 1982, Stratigraphic and structural framework of the Challis volcanics in the eastern half of the Challis 10′ × 20′ quadrangle, Idaho, *in* Bonnichsen, W., and Breckenridge, R.M., eds., Cenozoic Geology of Idaho: Idaho Bureau of Mines and Geology, Bulletin 26, p. 3–22.

McKee, T.M., 1970, Preliminary report on fossil fruits and seeds from the mammal quarry of the Clarno Formation, Oregon: Ore Bin, v. 32, p. 117–132.

Merriam, J.C., 1901a, A geological section through the John Day Basin: The Journal of Geology, v. 9, p. 71–72.

Merriam, J.C., 1901b, A contribution to the geology of the John Day Basin: The Journal of Geology, v. 9, p. 269–314.

Miyashiro, A., 1974, Volcanic rock series in island arcs and active continental margins: American Journal of Science, v. 274, p. 321–355.

Moye, F.J., Hackett, W.R., Blakely, J.D., and Snider, L.G., 1988, Regional geologic setting and volcanic stratigraphy of the Challis volcanic field, Central Idaho, *in* Link, P.K, and Hackett, W.R., eds., Guidebook to the geology of central and southern Idaho: Idaho Geological Survey, Bulletin 27, p. 87–97.

Obermiller, W.A., 1987, Geologic, structural, and geochemical features of basaltic and rhyolitic volcanic rocks of the Smith Rock–Gray Butte area, central Oregon [M.S. thesis]: Eugene, University of Oregon, 169 p.

Peck, D.L., 1964, Geologic reconnaissance of the Antelope-Ashwood area of north-central Oregon, with emphasis on the John Day Formation of late Oligocene and early Miocene age: U.S. Geological Survey Bulletin 1161-D, 26 p.

Retallack, G.J., Bestland, E.A., and Fremd, T.J., 2000, Eocene and Oligocene paleosols of Central Oregon: Geological Society of America Special Paper 344, 192 p.

Retallack, G.J., Orr, W.N., Prothero, D.R., Duncan, R.A., Kester, P.R., and Ambers, C.P., 2004, Eocene-Oligocene extinction and paleoclimatic change near Eugene, Oregon: Geological Society of America Bulletin, v. 116, p. 817–839, doi: 10.1130/B25281.1.

Riddihough, R., Finn, C., and Couch, R., 1986, Klamath–Blue Mountain lineament, Oregon: Geology, v. 14, p. 528–531, doi: 10.1130/0091-7613(1986)14<528:KMLO>2.0.CO;2.

Robinson, P.T., 1969, High-titania alkali-olivine basalt of north-central Oregon: Contributions to Mineralogy and Petrology, v. 22, p. 349–360, doi: 10.1007/BF00400129.

Robinson, P.T., 1975, Reconnaissance geologic map of the John Day Formation in the southwestern part of the Blue Mountains and adjacent areas, north-central Oregon: U.S. Geological Survey Miscellaneous Investigations Map I-872, scale 1:125,000.

Robinson, P.T., and Brem, G.F., 1981, Guide to geologic field trips between Kimberly and Bend, Oregon with emphasis on the John Day Formation, *in* Johnston, D.A., and Donnelly-Nolan, J., eds., Guides to some volcanic terranes in Washington, Idaho, Oregon, and northern California: U.S. Geological Survey Circular 838, p. 41–58.

Robinson, P.T., and Stensland, D., 1979, Geologic map of the Smith Rock area, Oregon: U.S. Geological Survey Miscellaneous Investigations Map I-1142, scale 1:48 000.

Robinson, P.T., Brem, G.F., and McKee, E.H., 1984, John Day Formation of Oregon: a distal record of early Cascade volcanism: Geology, v. 12, p. 229–232, doi: 10.1130/0091-7613(1984)12<229:JDFOOA>2.0.CO;2.

Robinson, P.T., and Walker, G.W., and McKee. E.H., 1990, Eocene(?), Oligocene, and lower Miocene rocks of the Blue Mountains region, *in* Walker, G.W., ed., Geology of the Blue Mountains region of Oregon, Idaho, and Washington: U.S. Geological Survey Professional Paper 1437, p. 13–27.

Rogers, J.W., and Novitsky-Evans, J.M., 1977, The Clarno Formation of central Oregon, U.S.A., volcanism on a thin continental margin: Earth and Planetary Science Letters, v. 34, p. 56–66, doi: 10.1016/0012-821X(77)90105-4.

Self, S., Goff, G., Gardner, J. N., Wright, J. V., and Kite, W. M., 1986, Explosive rhyolitic volcanism in the Jemez Mountains: vent locations, caldera development, and relation to regional structure: Journal of Geophysical Research, v. 91B, p. 1,779–1,798.

Sherrod, D.R., Taylor, E.M., Ferns, M.L., Scott, W.E., Conrey, R.M., and Smith, G.A., 2004, Geologic map of the Bend 30′ × 60′ quadrangle, central Oregon: U.S. Geological Survey Geologic Investigations Series I-2683, 48 p., scale 1:100,000.

Silberling, N.J., Jones, D.L., Blake, M.C., Jr., and Howell, D.G., 1984, Lithotectonic terrane map of the western conterminous United States, part C, *in* Silberling. N.J. and Jones, D.L., eds., Lithotectonic terrane maps of the North American Cordillera: U.S. Geological Survey Open-File Report 84-523, 43 p.

Smith, G.A., Sherrod, D.R., Ferns, M.L., and Lite, K., 1996, Geology of the Opal City 7.5′ quadrangle, Deschutes and Jefferson Counties, Oregon: Oregon Department of Geology and Mineral Industries unpublished map, scale 1:24,000.

Smith, G.A., Manchester, S.R., Ashwill, M., McIntosh, W.C., and Conrey, R.M., 1998, Late Eocene–early Oligocene tectonism, volcanism, and floristic change near Gray Butte, central Oregon: Geological Society of America Bulletin, v. 110, p. 759–778, doi: 10.1130/0016-7606(1998)110<0759:LEEOTV>2.3.CO;2.

Smith, R.L., and Bailey, R.A., 1968, Resurgent cauldrons, *in* Coats, R.R., et al. eds., Studies in Volcanology: A Memoir in Honor of Howell Williams: Geological Society of America Memoir 116, p. 613–662.

Steven, T.A., and Lipman, P.W., 1976, Calderas of the San Juan volcanic field, southwestern Colorado. U.S. Geological Survey Professional Paper 958, p. 1–35.

Stewart, J.H., and Carlson, J.E., 1976, Cenozoic rocks of Nevada—Four maps and brief description of distribution, lithology, age, and centers of volcanism: Nevada Bureau of Mines and Geology, Map 52, 5 p., scale 1:100,000.

Swanson, D.A., 1969, Reconnaissance geologic map of the east half of the Bend quadrangle, Crook, Wheeler, Jefferson, Wasco, and Deschutes Counties, Oregon: U.S. Geological Survey Miscellaneous Investigations Map I-568, scale 1:250,000.

Swanson, D.A., and Robinson, P.T., 1968, Base of the John Day Formation in and near the Horse Heaven mining district, north-central Oregon: U.S. Geological Survey Professional Paper 600-D, p. D154–D161.

Taylor, E.M., 1981, A mafic-dike system in the vicinity of Mitchell, Oregon, and its bearing on the timing of Clarno-John Day volcanism and early Oligocene deformation in central Oregon: Oregon Geology, v. 43, p. 107–112.

Thompson, M.L., and Wheeler, H.E., 1942, Permian fusulinids from British Columbia, Washington, and Oregon: Journal of Paleontology, v. 16, p. 700–711.

Thormahlen, D., 1984, Geology of the northwest quarter of the Prineville quadrangle [M.S. thesis]: Corvallis, Oregon State University, 116 p.

Urbanczyk, K.M., 1994, Geology of the eastern part of the Clarno Formation, northeast Oregon [Ph.D. dissertation]: Pullman, Washington State University, 230 p.

Vance, J.A., 1988, New fission track and K-Ar ages from the Clarno Formation, Challis-age volcanic rocks in north-central Oregon: Geological Society of America Abstracts with Programs, v. 20, no. 6, p. A473.

Waters, A.C., 1966, Stein's Pillar area, central Oregon: Ore Bin, v. 28, p. 137–144.

Waters, A.C., Brown, R.E., Compton, R.R., Staples, L.W., Walker, G.W., and Williams, H., 1951, Quicksilver deposits of the Horse Heaven Mining District, Oregon: U.S. Geological Survey Geologic Bulletin 969-E, 149 p., 21 pl.

Walker, G.W., and Robinson, P.T., 1990, Paleocene (?), Eocene, and Oligocene (?) rocks of the Blue Mountains region, *in* Walker, G.W., ed., Geology of the Blue Mountains region of Oregon, Idaho, and Washington: U.S. Geological Survey Professional Paper 1437, p. 29–62.

White, J.D.L., and Robinson, P.T., 1992, Intra-arc sedimentation in a low-lying marginal arc, Eocene Clarno Formation, central Oregon: Sedimentary Geology, v. 80, p. 89–114, doi: 10.1016/0037-0738(92)90034-O.

Williams, H., 1957, A geologic map of the Bend quadrangle and a reconnaissance geologic map of the central portion of the High Cascade Mountains: Oregon Department of Geology and Mineral Industries map (unnumbered series), scale 1:250,000.

Manuscript Accepted by the Society 15 July 2009

Printed in the USA